Science Translational Medicine
AAAS

Supplementary Materials for

Cis P-tau underlies vascular contribution to cognitive impairment and dementia and can be effectively targeted by immunotherapy in mice

Chenxi Qiu *et al.*

Corresponding author: Kun Ping Lu, klu@bidmc.harvard.edu; Xiao Zhen Zhou, xzhou@bidmc.harvard.edu

Sci. Transl. Med. **13**, eaaz7615 (2021)
DOI: 10.1126/scitranslmed.aaz7615

The PDF file includes:

Other Supplementary Material for this manuscript includes the following:

Supplementary Materials:

Supplementary Materials and Methods

Animals

Mice were housed in-group cages (n = 5 per cage) containing bedding covering the floor, overhead storage of food pellets, and a water bottle for the mice to feed and drink freely. The animal facility where the mice were housed was maintained at a constant temperature and humidity, and the animals were subject to a standard 12-hour light-dark cycle. All animals used were male in order to control for changes to cognition occurring in different hormonal states in female mice. All experiments comply with the relevant guidelines and regulations regarding the care and use of animals for experimental procedures in accordance with the standards of International Animal Care and Use Committee, and the Beth Israel Deaconess Medical Center Animal Care and Use Committee.

Cell cultures

SH-SY5Y neuroblastoma cells. SH-SY5Y cells were cultured in Dulbecco's modified Eagle's medium (DMEM) containing 10% fetal calf serum. The media were supplemented with 100 Units/ml penicillin/steptomycin. Purified *cis* P-tau (0.2, 0.4 or 0.8 μg/μl) or recombinant human tau (3.2 μg/μl) or vehicle (HEPES-saline solution) were applied to culture cell lines for 48h, and subsequently treated with *cis* or *trans* mAbs at 8.0 μg ml−1 once 1h after application, and the cell viabilities were examined (*12, 13*).

Primary neurons. Primary neurons were prepared from 17-day-old embryonic mouse brain cerebral cortex of either sex. Dissected cortices transferred to Neurobasal medium (Invitrogen) supplemented with 2% B27 (Invitrogen), 2 mM glutamine (Invitrogen), and antibiotics were

mechanically dissociated into single cells. The dissociated cells were cultured in Neurobasal medium supplemented with 2% B27, 2 mM glutamine, antibiotics, human recombinant epidermal growth factor (EGF; 20 ng/ml) (Invitrogen), and human recombinant basic fibroblast growth factor (bFGF; 20 ng/ml) (Invitrogen). Glass coverslips were coated with poly-l-lysine (15 μg/ml) (Sigma) and laminin (5 μg/ml) (Sigma) and were placed in 24-well plates. Primary neurons were pretreated with 20 or 40 μM z-VAD-fmk for 30 min, and subsequently treated with 6 nM purified *cis* P-tau for 24, 48, 72, 96 h and the cell viabilities were examined. The negative control group was treated with an equal concentration of the HEPES-saline solutions, as described (*12*)

Live/Dead Cell Viability Assay. Cell viabilities were examined using Live and Dead cell assay kit (Abcam). After staining cells with the Live and Dead Dye diluted to 5X concentration in PBS, cells were incubated for 10-min at room temperature in the dark. Immunostaining images were then quantified using Fiji/ImageJ Coloc 2 (*12, 13*).

Purification of soluble *cis* P-tau from acute TBI mouse brains and recombinant tau from *E.coli DE3*

We used *cis* mAb affinity chromatography to purify *cis* P-tau from brains of injured htau mice with closed head injury model (n=20), as previously described (*12*). Two-month-old htau mice obtained from the Jackson Laboratories underwent repetitive mild injuries (rmTBI, 7 injuries in 9 days), followed by preparation of brain cortex tissue lysate at 2 weeks after injury, when it is known to contain robust *cis* P-tau without other commonly known tau changes, including tau oligomerization, aggregation and tangle-related epitopes (*12, 13*). The recombinant human full-length tau isoform was expressed in DE3 bacteria and purified by Ni-NTA column as previously described (*9*). Briefly, *E.coli* DE3 with His tagged human tau expressed in pET28 plasmid were grown at 37˚C until OD reaches 0.6-1, followed by induction of recombinant tau with 0.5mM

IPTG for 16 hours at 16˚C. Cells were resuspended and sonicated in the lysis buffer (50mM Tris-HCl, pH=8; 500mM NaCl, 5% glycerol, 1% triton), as described (*9*). The lysate is loaded to the Ni-NTA column, followed by three times of washes using lysis buffer and eluted with elution buffer (50mM Tris-HCl, pH=8; 500mM NaCl, 5% glycerol, 250mM imidazole). The protein concentrations of *cis* P-tau and recombinant tau were estimated by the Bio-Rad DC Protein Assay kit. Purified proteins were aliquoted and stored at -80˚C.

Stereotaxic surgery

3-month-old wild-type C57BL/6 or Tau KO mice were deeply anesthetized with isoflurane, immobilized in a stereotaxic frame (David Kopf Instruments) and bilaterally inoculated with recombinant human total tau protein or purified *cis* P-tau in the overlying cortex (from bregma: 0.0 mm posterior, ±2 mm lateral, -0.8- & -1.0-mm ventral) using a Hamilton syringe under aseptic conditions. Each of the four injection sites (two injections to each hemisphere; -0.8- & -1.0-mm ventral) received 2µl of inoculum, with recombinant human tau at 0.4 µg/µl (0.8 µg tau/site), or purified *cis* P-tau 0.1 µg/µl (0.2 µg tau/site), or vehicle PBS, and materials were injected into the lower layer of cortex first (-1.0-mm ventral) before the needle was pulled upper layer of the cortex (-0.8-mm ventral). The body temperature of the mice was maintained at 37 °C during and after surgery until were awake. To examine time-dependent behavioral and pathological changes, mice were analyzed at 1- and 10-months post-injection. As a proof of causality, another set of mice were randomized to treatment with *cis* p-tau monoclonal mouse antibody (clone #113) or mouse IgG2b in a double-blind manner, and received 1 dose of *cis* antibody or IgG2b (control) intraperitoneal (i.p. 200 micrograms per mouse) pre-treatment 3 days before the surgery, and three following days after the surgery, and continued 3 months weekly and biweekly over 5 months (with total 5 months

of treatment). Mice were analyzed at 1- and 10-months post-injection as described in the text.

BCAS Surgery

BCAS surgery was performed as previously described (*22*). Briefly, mice were anesthetized with isoflurane. Both common carotid arteries were carefully isolated from vagal nerves through a midline cervical incision. A microcoil (Sawane Spring Co.) with a 0.18 mm diameter was applied by rotating it around the bilateral common carotid artery. Body temperature was monitored and maintained between 36.5 and 37.5 °C with a heating blanket. After applying microcoil, the incision was closed with a silk suture, and mice were put on a heating blanket after surgery. The sham-operated mice underwent the same procedure without microcoil placement.

Antibody treatment

Mice were randomized to treatment with *cis* p-tau monoclonal mouse antibody (clone #113) or mouse IgG2b in a double-blind manner. Three-month-old htau mice received *cis* antibody or IgG2b intraperitoneal (i.p.) treatment (200 μg) weekly for the first 4 months and continued biweekly for the next 4 months; or 13-month-old htau mice received *cis* antibody or IgG2b intraperitoneal (i.p.) treatment (200 μg) weekly for 6 months, as described in the text, followed by analyses at 11 or 19 months (with total 8 and 6 months of treatment, respectively). For BCAS model, mice received 300 μg i.p every 3-day at first 2 weeks, continued by 150 μg i.p weekly, followed by analysis at 7, 14, 28 and 180 days after surgery. For all behavioral tests, experimenters were blinded to injury and treatment status, using color-coding stored in a password-protected computer, as described (*12, 13*).

Electron Microscopy

Mice were perfused with a fixative solution, a mixture of 15% picric acid (13% saturated solution;

Sigma), 4% paraformaldehyde (Electron Microscopy Sciences), and 0.1% glutaraldehyde (electron microscopy grade 50% solution; Electron Microscopy Sciences) dissolved in PEM buffer (0.1 M PIPES, pH 7.2, 1 mM EGTA, 1 mM MgCl2). Perfused brains were removed, sliced and kept in the same fixative for further 4h at 4 °C. The samples were processed for electron microscopic observation. Specimens were examined with a JEM-1010 transmission electron microscope (JEOL) (*12*).

Multielectrode array (MEA) synaptic recordings

Mice were anaesthetized with isoflurane (NDC 10019-360-40, Baxter Healthcare Corporation) and decapitated. The brains were quickly removed and placed for sectioning in ice-cold treatment artificial cerebrospinal fluid (tACSF) containing (in mM) NaCl 124, KCl 3, NaH2PO4 1.25, NaHCO3 26, CaCl2 2, MgSO4 2, and glucose 10 (pH 7.4, and bubbled with 95% O2 and 5% CO2 gas mixture). Cortical slices (thickness 350 μm) were cut with a Vibratome 1000P (Leica VT1000P, Leica Microsystems Inc.) and transferred to a chamber with oxygenated tACSF for 90 min at 30 °C before recording. Field excitatory postsynaptic potentials (fEPSP) were recorded using a multi-electrode array recording system (MED64 system) with MED-P5155 probe (AutoMate Scientific, Inc.) in this study. After incubation, one cortical slice was positioned in the center of the MED64 probe (to fully cover the 8 × 8 electrode array) with oxygenated recording ACSF (rACSF) containing (in mM) 124 mM NaCl, 3 mM KCl, 1.25 mM NaH2PO4, 26 mM NaHCO3, 2 mM CaCl2, 1 mM MgSO4, and 10 mM glucose (pH 7.4) at 30°C. A fine nylon mesh and a mesh anchor were placed on top of the slice to immobilize the slice during recording. The probe with immobilized slice was connected to two MED64 amplifiers (MED64 Head Amplifier (MED-A64HE1) and Main Amplifier (MED-A64MD1), AutoMate Scientific, Inc.). The slice was continuously perfused with oxygenated, fresh rACSF at

the rate of 2 ml min−1 using a peristaltic pump (Minipuls 3, Gilson Inc.). Data was collected using Mobius software (Mobius 0.4.2). Field potentials were induced by single pulses (0.2 ms) delivered at 0.05 Hz through one planar microelectrode in layer V of cortical slice. We used stimulus intensity sufficient to induce a 50% of the maximal fEPSP slope in all experiments. The fEPSP was recorded from the channels in layer II/III. A stable fEPSP slope for at least 20 min was recorded as baseline. The induction protocol of LTP that we used is 5 Hz theta burst (each burst consists of 4 pulses at 100 Hz). The data were filtered at 10 kHz and digitized at a 20 kHz sampling rate. Data were analyzed offline by the MED64 Mobius software. For quantifying the LTP, the mean of fEPSP slope (10–40%) within the last 10 min of recording was normalized and expressed as a fold change of the averaged baseline (first 10 min of the baseline), as described (*12*).

Western blot

Immunoblotting analysis was carried out as described (*13*). Briefly, brain tissues were lysed in RIPA buffer (50 mM Tris-HCl, pH 7.4, 150 mM NaCl, 2 mM EDTA, 1% NP 40, 0.1% SDS, 0.5% Na-deoxycholate, 50 mM NaF) containing proteinase inhibitors and then mixed with SDS sample buffer and loaded onto a gel after boiling. The proteins were resolved by polyacrylamide gel electrophoresis and transferred to PVDF membrane. After blocking with 5% milk in TBST (10 mM Tris-HCl pH 7.6, 150 mM NaCl, 0.1% Tween 20) for 1 h, the membrane was incubated with primary antibody (*cis* mAb) (*12*), Tau5 (Biosource Camarillo), cleaved caspase-3 (Asp175) (Cell Signaling) and actin antibodies (Sigma) in 5% milk in TBST overnight at 4 °C. Then, the membranes were incubated with HRP-conjugated secondary antibodies in 5% milk in TBST. The signals were detected using chemiluminescence reagent (Perkin Elmer).

Immunostaining Analysis

Immunostaining analysis was carried out as described (*12-14*). The primary antibodies used were *cis* mAb (#113 or #74) (*12*), tau tangle-related mAbs AT8, AT100 (Innogenetics), anti-tau rabbit mAb (E178, Abcam), anti-neurofilament mouse mAb (SMI-312, IgG1, Abcam) for labeling axons, CNPase monoclonal (11-5B) antibody (ab6319, Abcam) and MBP antibody (ab40390, Abcam) for labeling myelin, GST-π Polyclonal antibody (MBL Life Science), Iba1 polyclonal antibody (Wako) for microglia, GFAP polyclonal antibody (BioGenex) for astrocytes, cleaved caspase-3 (Asp175) (Cell Signaling) antibody for activated caspase-3, beta-tubulin monoclonal antibody (ab179513, Abcam) for labelling beta-tubulin, TPPP/P25 monoclonal antibody (Enzo Life Science, 803-342-C100) for labelling TPPP/P25, FKBP4/52 monoclonal antibody (ab129097, Abcam) for labelling FKBP4/52, ApoE monoclonal antibody (ab183597, Abcam) for labelling ApoE, Caprin2 polyclonal antibody (ab122583, Abcam) for labelling Caprin2, Synapsin1 polyclonal antibody (ab64581, Abcam) for labelling Synapsin1 and anti-NeuN AF488-conjugated monoclonal antibody (Millipore) for labeling neurons. After treatment with 0.3 % hydrogen peroxide, slides were briefly boiled in 10mM sodium citrate, pH 6.0, for antigen enhancement. The sections were incubated with primary antibodies overnight at 4°C. Then, biotin-conjugated secondary antibodies (Jackson ImmunoResearch), streptavidin-conjugated HRP (Invitrogen) were used to enhance the signals. For double immunofluorescence staining, the sections were incubated with Alexa Fluor 488 or 568 conjugated isotype-specific secondary antibodies (Jackson ImmunoResearch), or IRDye™ 800CW conjugated donkey anti-rabbit IgG (H+L) (Rockland Immunochemicals) for 1 h at room temperature. Manufacturer-supplied blocking buffer (Invitrogen) was used for each reaction. The sections were washed 4 times with TBS after each step. Labeled sections were visualized with a Zeiss confocal microscope or with the LI-COR Odyssey (21 μm resolution, 1mm offset). The gain of the confocal laser was set at the threshold

where there are no fluorescence signals including autofluorescence in sections without primary antibody but with secondary antibody. Immunostaining images and their intensity were quantified using Fiji/ImageJ Coloc 2, as described (*12-14*).

Gallyas silver staining

For Gallyas silver staining a kit of FD NeuroSilver (FD NeuroTechnologies) was used following the instructions of the manufacturer, as described (*13*). The Optical Density was measured using Fiji/ImageJ Coloc 2.

Thioflavin-S staining

For thioflavin-S staining a substance (Sigma-Aldrich) was used following the instructions of the manufacturer.

Luxol-fast blue staining

For Luxol-fast blue staining a kit of FD Luxol Fast Blue (FD NeuroTechnologies) was used following the instructions of the manufacturer. The Optical Density was measured using with Fiji/ImageJ Coloc 2.

Behavioral tests

All the tests were conducted from 10:00am-03:00pm in the lights-on cycle at BIDMC Animal Research Facility or Harvard Mouse NeuroBehavior Laboratory by experimenters blinded to group designation. Mice were habituated to the procedure room 30 min before each test.

Novel object location recognition test. The Novel object location recognition test consisted of an open field-box (44 cm x 44 cm x 44 cm). The habituation period was 10 minutes daily of free exploration in the arena without objects over 3 days. On test day the animals were allowed to explore three identical objects (with same color Lego sets) placed into the area in fixed location

for 5 minutes and the time spent inspecting the individual objects was recorded (Noldus Ethovision XT). Without any time-interval the animals were replaced into the box where one object was placed into a new location the mice were allowed to explore them for an additional 3 minutes. The floor was covered with sawdust (1 cm deep, used and saturated with the odor of the animals) during habituation and test trials. The discrimination ratio for the novel object location of the object was analyzed as previously described (*13*).

Bright-Light Open Field test. Mice will be placed in the center of a brightly lit (200–300 lux) chamber of the open-field apparatus (44x44x30 cm). Movements of the animals is tracked by an automatic monitoring system for 5 min. A computer-assisted video-tracking system (Noldus Ethovision) recorded horizontal motor (distance traveled) and central activity (distance traveled in central area/ total distance traveled).

T-maze. The mice were habituated to a white plastic T-maze (with a stem section and two sample arms section, all of them are 30 x 10 cm with a 15-cm-high wall) for 10 min on day 1. One day after the habituation session was complete, mice were subjected to a left-right discrimination task, with 4 trials for each mouse. In the sample phase, the mice were placed in the start arm with Guillotine door closed for 10 s, and then open the door to let the mice explore the maze with one sample arm is guillotine door for this arm was closed to make the mice stay in the arm for 10 s. Next, in the choice phase, the mice were placed in the start arm again for 10 s, and then explored the whole maze without any guillotine doors closed. The goal arm (correct arm) or the opposite arm (wrong arm), which the mice first went in, was recorded. The intra-trial interval between the sample phase and choice phase was 30 min for htau mice and 10 s for BCAS mice. The inter-trial interval between each trial was 1 hr. The percent correct choices for each mouse were calculated.

Elevated plus maze. The elevated plus maze was used to assess anxiety/risk-taking behavior two

months after injury and carried out as described (*12*). Briefly, the elevated plus maze consists of two white open arms (30 x 5 cm) and two white closed arms of the same size with 15-cm-high walls, extended out opposite from each other from a central platform (decision zone) to create a plus shape. The entire apparatus is raised 38 cm above the floor (Lafayette Instruments). Mice are placed on the center platform of the maze, facing a closed arm, and allowed to explore the apparatus for 5 min. The maze is cleaned between subjects with a weak ethanol solution and dried. A computer-assisted video-tracking system (Noldus Ethovision) recorded the total time spent in the center platform (decision zone), and the two closed or 'safe' arms and the two open or 'aversive' arms.

Accelerated Rotarod. The mice were placed in the rotating cylinder 4 times per day for three consecutive days totally. Each trial lasts a maximum of 10 min, during which time the rotating rod accelerated from 4 to 40 r.p.m. over the first 5 min of the trial and then remained at the maximum speed for the remaining 5 min. Animals were rested for at least 10 min between trials to avoid fatigue and exhaustion.

Morris Water maze. A Morris water maze (MWM) paradigm was used to evaluate spatial learning and memory, as described (*12*). The apparatus consisted of a white pool (83 cm diameter, 60 cm deep) with water filled to 29 cm depth, at ~24 °C. Intra-maze and extra-maze cues were included. The target (a round, clear, plastic platform 10 cm in diameter) was placed 1 cm below the surface of the water. During hidden and visible platform trials, mice were randomized to one of four starting quadrants. Mice were placed in the tank facing the wall and allocated 90 s to find the platform, mount the platform, and remain on it for 30 s. Mice were then dried under a heat lamp before their next run. The time until the mouse mounted the platform (escape latency) was recorded. Mice that did not mount the platform in the allocated 90 s were guided to the platform

by the experimenter and allowed 30 s to become acquainted with its location. On each training day, mice received three training trials, with a 45-minute break between trials. For visible platform trials, a red reflector was used to mark the top of the target platform. For probe trials, mice were placed in the tank with the platform removed and given 60 s to explore the tank. Noldus Ethovision software tracked swim speed, total distance moved, and time spent in the target quadrant where the platform was previously located.

Contextual Fear Conditioning test. Contextual Fear conditioning (CFC) was used to assess memory and was based on the tendency of mice to show a fear response (freezing) when re-exposed to the context where they received a foot shock. Fear conditioning was performed in a specialized chamber of dimensions: [Interior: 30.5 x 24.1 x 21 cm; Exterior: 31.8 x 25.4 x 26.7 cm; Channels (six, three per wall): 7.62 cm], containing a shock grid floor, speaker and video camera. After each animal the chamber was cleaned with an ethanol solution to remove any scent left behind by previous animals. For conditioning, the chamber was equipped with a shock pad. Conditioning consists of a 2-minute acclimation period, followed by two consecutive 2-minute fear conditioning trials consisting of a 2 seconds shock (0.5 mA) at the end of each interval. Mice were removed from the chamber 1 min after the last foot shock (total 7 minutes) and returned to their home cages. The mouse's fear response was recorded during the CS presentations. "Freeze" time was recorded both prior to and following the shock presentation. Twenty-four hours after the training session, mice were placed back into the conditioning chamber for 3 min (no electric shock was delivered during this session) and freezing was videotaped and scored with Topscan software (CleverSys). Mice were constantly monitored during the course of the experiment. The freezing response was used as a surrogate marker of memory performance because mice remembering receiving the shock during the training session were expected to spend a significant amount of

time freezing during the retention session.

Single-nucleus RNA-seq sample preparation

Three mice from each group (Sham, BCAS followed by IgG treatment, BCAS followed by *cis* mAb treatment) were subjected to single-nucleus preparations. Cortical tissue was dissected from mice perfused with cold PBS buffer with a previously described transcription inhibitor cocktail at a speed of 6 mL/min for 8 minutes and flash frozen in liquid nitrogen (*45*). The frozen tissue was subsequently placed into a tissue dounce for homogenization with homogenization buffer (0.25M sucrose, 25mM KCl, 5mM $MgCl_2$, 20mM Tricine-KOH pH7.8 with freshly added 1mM DTT, 0.15mM spermine (Sigma), 0.5mM spermidine (Sigma), 0.04% BSA (Sigma) and RNase inhibitors (Promega). 5% IGEPAL (Sigma) stock solution was added to the homogenization buffer to a final concentration of 0.32% for 20 strokes with tight pestle. The homogenate was visually inspected, passed through 40-µm filter (BD Falcon) and layered onto an OptiPrep (Sigma) gradient. The gradient was centrifuged at 10,000g for 18 minutes, and nuclei were collected between the 30% and 40% OptiPrep gradient layers. Single nucleic suspension was visually confirmed under microscope and diluted to 80,000 nuclei/mL for nuclei encapsulation and sequencing library preparation done by Harvard Single Cell Core following an inDrop protocol as previously described (*48*). The prepared libraries are sequenced on Illumina Nova-seq at Broad Institute Walk-up sequencing facility, at a coverage of about 7 billion reads for ~15,000 droplets (~450,000 reads per nuclei). Raw data are deposited under NCBI BioProject PRJNA521781.

Single-nucleus RNA-seq data quality controls and cell type cluster identification

Transcripts were mapped to the mouse transcriptome (GRCm38.81) following an established bioinformatics pipeline for inDrop experiments to create raw gene-cell counts matrices (Available on GEO: GSE126815) (*48*), with the slight modifications of adding an additional filtering step to

remove lower quality base calls using trimmomatic with the parameters "LEADING:28 SLIDINGWINDOW:4:26 MINLEN:15" after identifying abundant barcodes. Cells with low total raw counts were removed if they had fewer than a calculated number of counts. This trim threshold was based on the mode of the total counts for a given sample and was calculated as follows (eq1).

$$eq1 \begin{cases} If\ mode\_estimate < 100, trim\_threshold = mode\_estimate * 5.5 \\ If\ 100 \leq mode\ estimate \leq 450, trim\_thresold = (-0.01 * mode\_estimate) + 6.5 \\ If\ mode\_estimate > 450, trim\_threshold = mode\_estimate * 2 \end{cases}$$

Next, cells with library sizes more than three median absolute deviations (MADs) below the median library size were filtered out. Cells with a total number of expressed genes (>= 1 read) more than two MADs below the median total number of expressed genes were filtered out. Cells with a total percent of expressed genes originating from mitochondrial DNA more than six MADs above the median were filtered out. A doublet score was computed to estimate the percentage of barcodes for two or more cells as previously described (*49*), and cells with a doublet score of higher than 99% are excluded. Principle component analysis and t-Distributed Stochastic Neighbor Embedding (tSNE) analyses revealed no significant batch effects to be regressed out.

For the dimension reduction and cell-type identification, we used the Seurat package (v2.0) (*50*). Briefly, variable genes were identified by the FindVariableGene() function and principal component analysis was done by the RunPCA() function from Seurat package with parameters as previously described (*45*). The top 30 principal components were used for kNN clustering using the FindCluster() function, and similar clusters were combined by ValidateCluster() function using the following parameters (pc.use = 1, top.genes = 30, min. connectivity = 0.01, acc.cutoff = 0.9, verbose = TRUE). The top 30 principal components were subsequently used for t-distributed stochastic neighbor embedding (tSNE) by the RunTSNE() function. Cell types were identified by checking expression of well known brain cell type markers with the FeaturePlot() function, and

cross-validated by comparing the normalized expression profile of individual cells to the Mouse Cell Atlas (*51*). Additional distinct excitatory neuronal subtype markers are identified by FindAllMarkers() function with the parameters (only.pos = F, min.pct = 0.1, thresh.use = 0.25) and plotted. Dot plots and violin plots are generated using DotPlot() and VlnPlot() functions using default settings.

Differential gene expression analysis

Clusters of the same cell type were combined for differential gene expression analysis to provide sufficient coverage of genes and statistical power as previously described (*45*). We used Genewise Negative Binomial Generalized Linear Models (glmFit()) from the edgeR package for the differential gene expression analyses. Briefly, binomial dispersion was estimated using the estimateDisp(), followed by model fitting using glmFit() and finally, likelihood ratios for differential expression were calculated using glmLRT(). Differential gene expression results are provided in the supplemental data table (Table S2 and 4), including Log2 (fold change), p value and adjusted p value for false discovery rate (fdr). Heatmaps for Log2 (fold change) were generated using GENE-E from Broad Institute. In order to identify the top differentially expressed genes (DEGs) for each cell-type, p value < 0.01 threshold was taken when considered genes as differentially expressed for inhibitory neurons, astrocytes, oligodendrocytes and endothelia, while an additional cutoff fdr < 0.0001 is taken for excitatory neurons and all neurons. *Cis* mAb recovered genes are defined as genes that are differentially expressed between BCAS+IgG and sham but not differentially expressed between BCAS+*cis* and sham. Percentage of recovered genes is calculated as follows (eq2).

$$eq2\ Percentage\ of\ recovered\ genes = \frac{Number\ of\ recovered\ genes}{Number\ of\ differentially\ expressed\ genes}$$

Two-tailed Pearson correlation between tau concentration and percentage of recovered genes are computed using Graphpad Prism 6.

DEGs (p<0.01 for all cell types, except for excitatory neurons and all neurons with fdr adjusted p<0.0001 for excitatory neurons and all neurons) are subjected to Gene-ontology analyses using clusterProfiler and Gene set enrichment analysis against 4792 MSigdb C2 curated gene sets. Gene ontology terms that are too generic or too specific are filtered by the DropGO() functions of the clusterProfiler R package. Full list of GO terms significantly enriched in neuronal DEGs are provided in Table S3 and S5.

Supplementary figures

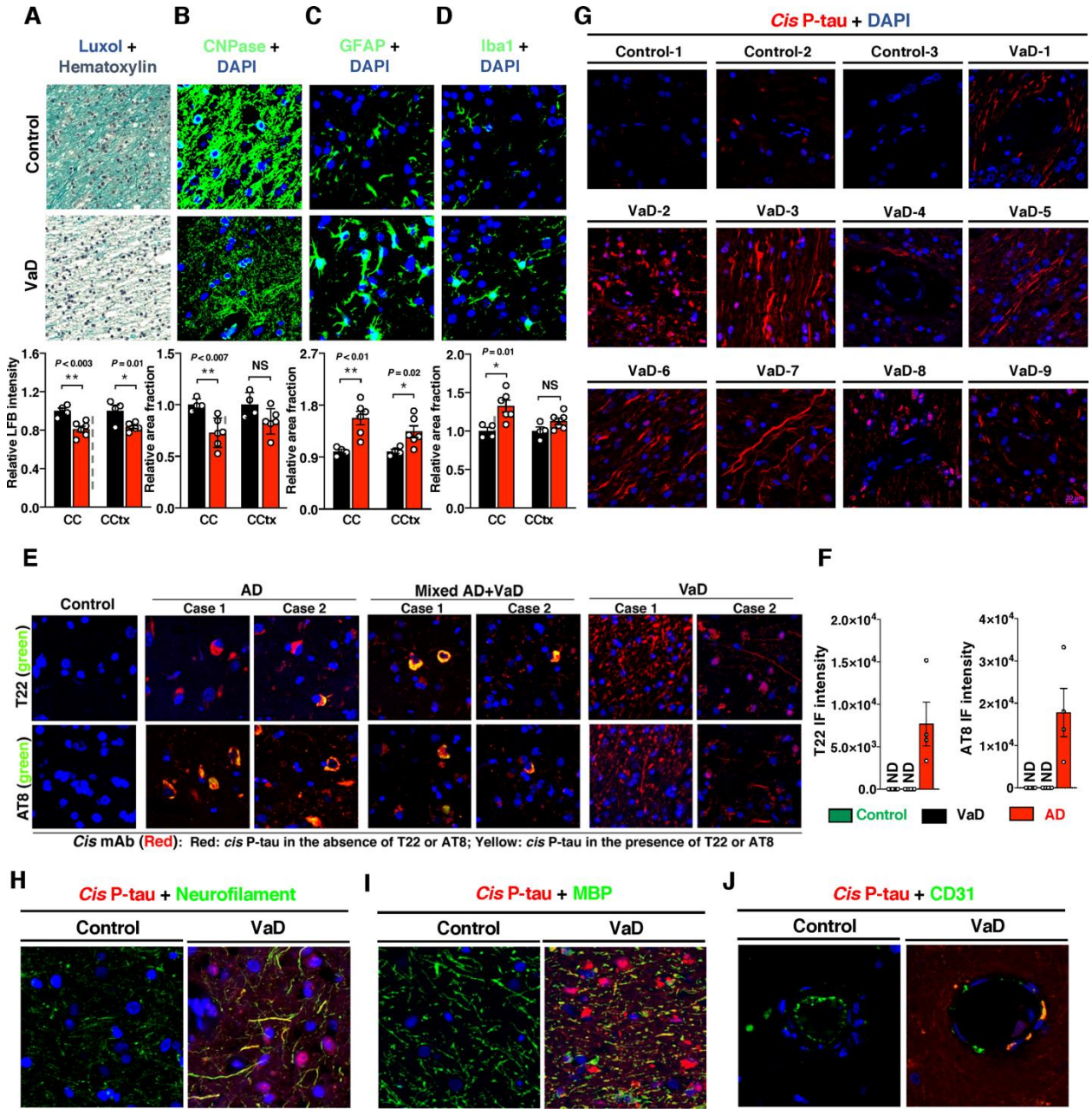

fig. S1. Demyelination, neuroinflammation and robust *cis* P-tau in the cingulate cortex overlaying the corpus callosum (CCtx-CC), and *cis* P-tau localization in neuronal axons, oligodendrocytes and microvascular endothelial cells in patient brains with VaD. (**A-D**) Brain sections of patients with VaD and healthy controls were subjected to Luxol fast blue and

hematoxylin staining (**A**), immunostaining with the oligodendrocyte marker CNPase (**B**), GFAP (**C**) and Iba1 (**D**). Upper, representative IF staining images in the corpus callosum; lower, quantitation and statistics for IF signal in the corpus callosum and the cingulate cortex. Black, control; Red, VaD; CC, corpus callosum; CCtx, cingulate cortex. NS, not significant. (**E** and **F**) IF staining of *cis* P-tau (*cis* mAb), tau oligomers (T22) and tangle epitopes (AT8) in the brain sections from the patients with AD, mixed AD/VaD and VaD, with age-matched healthy controls. (**G**) Brain sections from 9 patients with VaD and 3 age matched healthy controls are subjected to IF staining of *cis* P-tau with *cis* mAb. (**H-J**) Brain sections of patients with VaD and healthy controls were subjected to immunostaining with *cis* P-tau (red) and the neuronal axon marker neurofilament (green) (**H**), the oligodendrocyte marker MBP (green) (**I**) or the endothelial cell marker CD31 (green) (**J**), along with DAPI (blue). The data were presented as means ± SEM and the *p* values were calculated using unpaired two-tailed parametric Student's t-test. *, $p<0.05$, **, $p<0.01$.

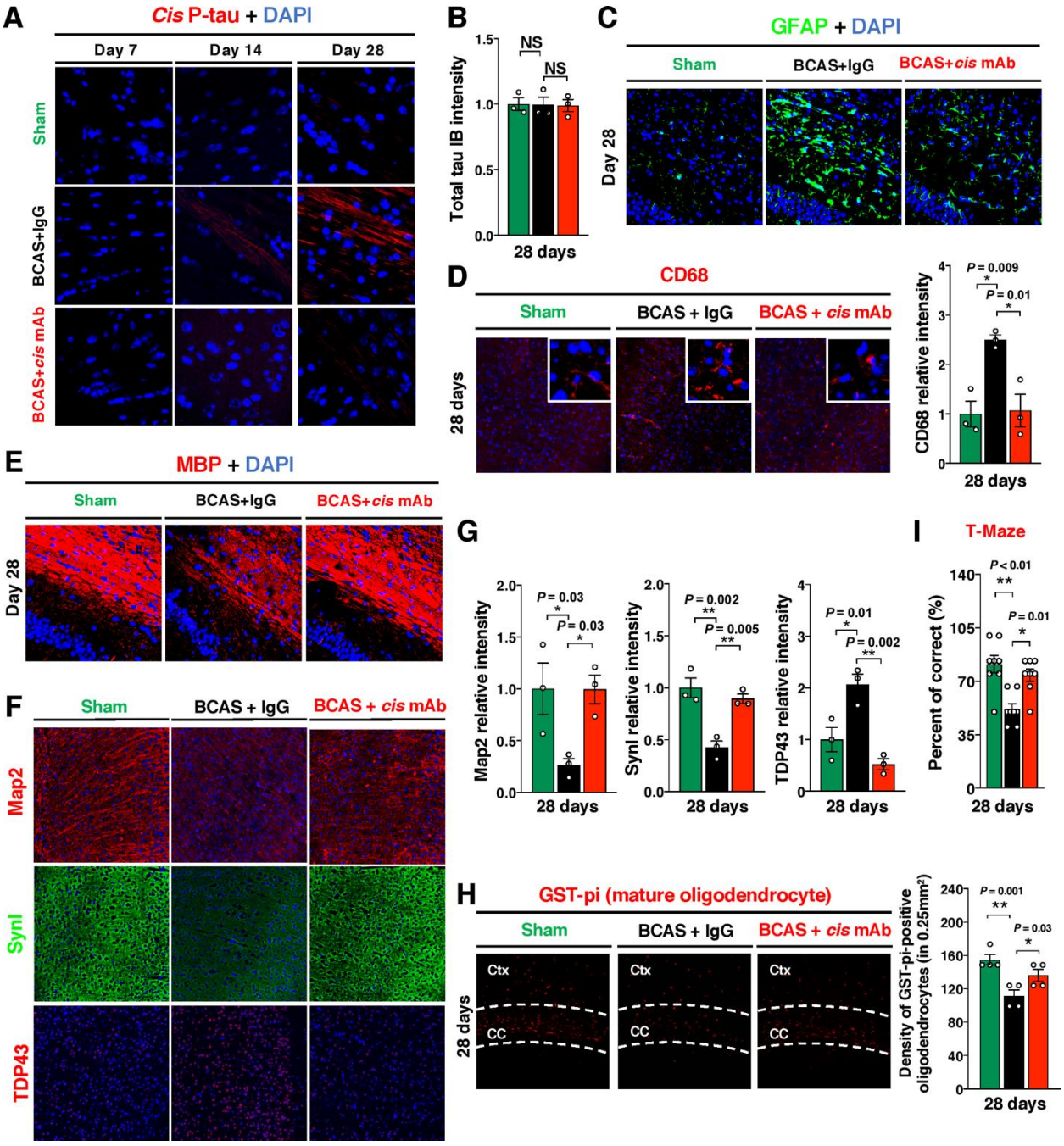

fig. S2. ***Cis*** **mAb treatment of BCAS mice eliminates** ***cis*** **P-tau induction and inhibits neuroinflammation, demyelination, and oligodendrocyte loss 28 days after surgery.**

(**A**) *Cis* P-tau IF staining in BCAS mice at 7, 14 and 28 days after surgery. (**B**) Quantitation of total tau IB intensity. (**C-H**) *Cis* mAb treatment effect of BCAS mice 28 days after surgery, as examined by IF staining of GFAP (**C**), microglia marker CD68 and quantitation (**D**), MBP (**E**), neuronal marker Map2, synapses marker Synapsin I, neurodegenerative marker TDP43 (**F**) and their quantitation (**G**), GST-pi-positive cells and quantitation (**H**). (**I**) *Cis* mAb treatment effect of working memory, as assessed by the percentage of correct choices in T maze. The data were presented as means ± SEM and the *p* values were calculated using one-way ANOVA with *post hoc* Dunnett's multiple comparison test. *, $p<0.05$; **, $p<0.001$; ***, $p<0.0001$.

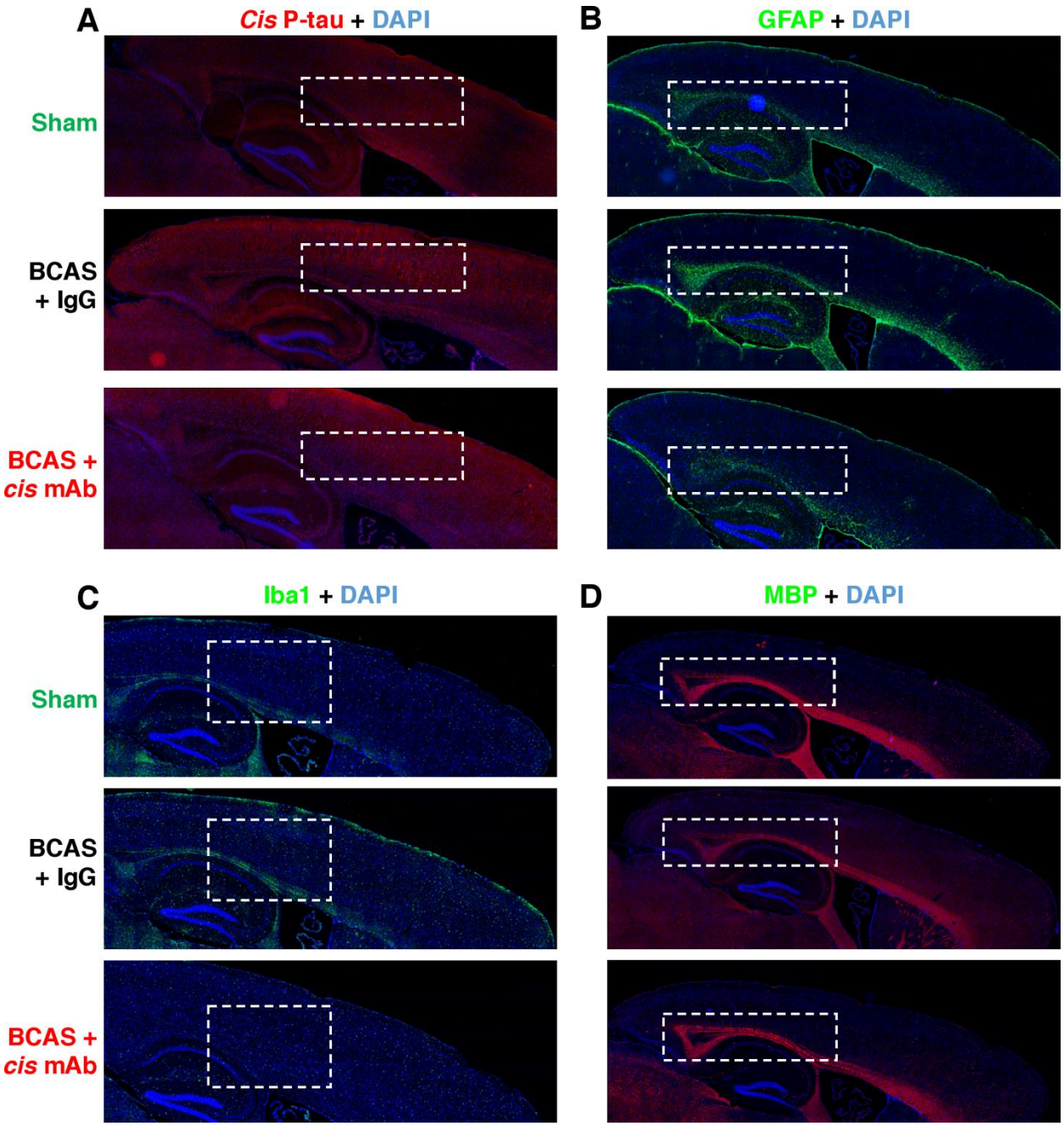

fig. S3. Robust *cis* P-tau is induced in the BCAS mice in the cortex overlaying corpus callosum, with increased GFAP, Iba1 and decreased MBP immunoreactivity. Low power images of *Cis* P-tau (**A**), GFAP (**B**), Iba1 (**C**) and MBP (**D**) immunoreactivity in the cortex and corpus callosum overlaying area.

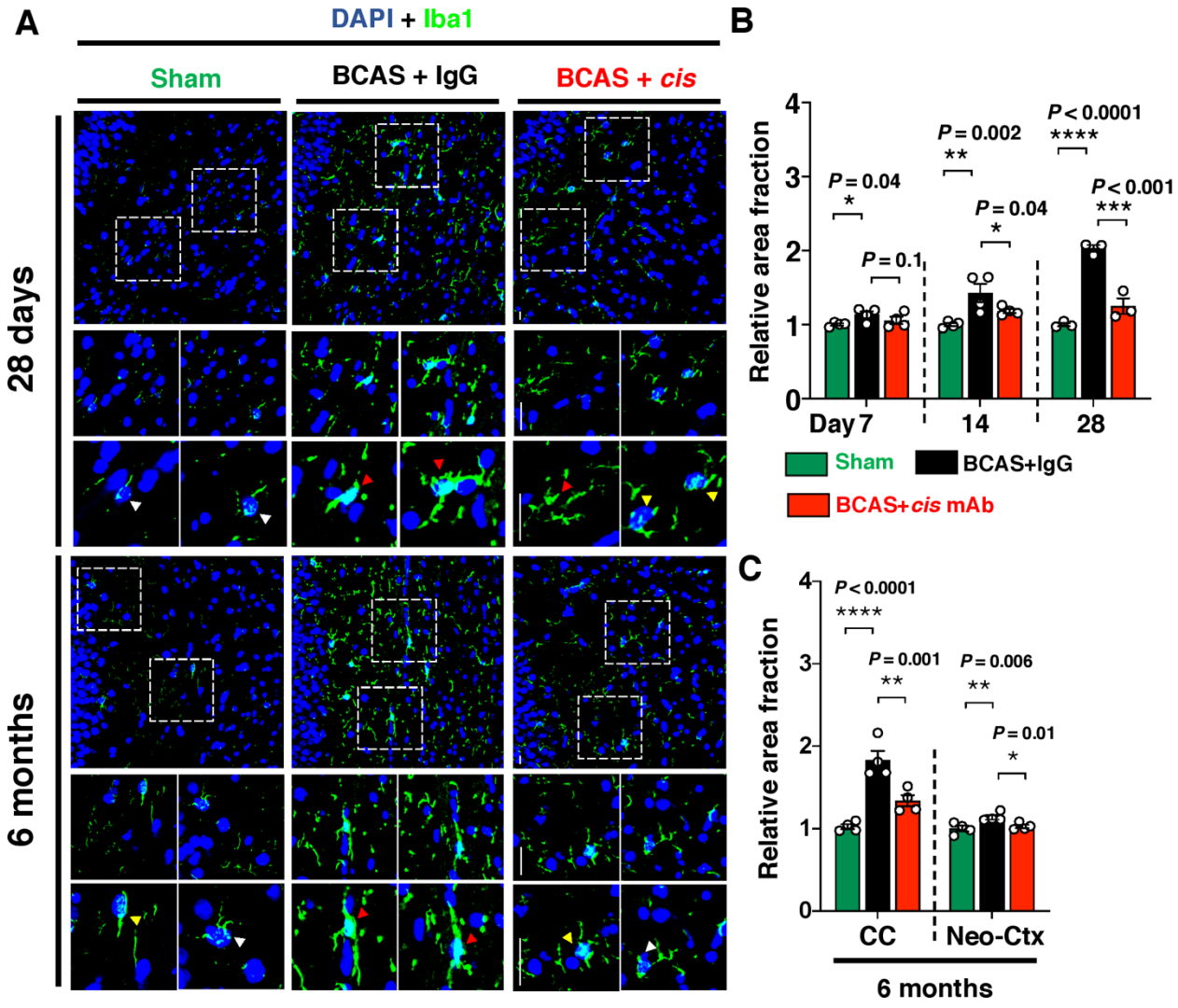

fig. S4. Microglial activation marker Iba1 is time dependently activated in the cortical region overlaying corpus callosum in BCAS mice and recovered by *cis* mAb for up to 6 month after surgery. **(A)** Representative micrographs of Iba-1 positive microglial cells depicting morphological stages of microglial activation ("ramified-resting" form - white arrow; "intermediate" form - yellow arrow; "amoeboid-activated" form - red arrow). Ramified form of microglia is characterized by thin processes with small cell bodies. Intermediate form of microglia are characterized by slightly thicker processes and enlarged cell bodies. Amoeboid form of microglia are characterized rounded macrophage-like morphology with no or few processes. (**B**

and **C**) Quantification of relative area fraction of Iba1 IF staining for 28 days and earlier (**B**) or 6 months (**C**) after BCAS are shown. The data were presented as means ± SEM and the *p* values were calculated using one-way ANOVA with *post hoc* Dunnett's multiple comparison test. *, $p<0.05$; **, $p<0.01$; ***, $p<0.001$; ****, $p<0.0001$.

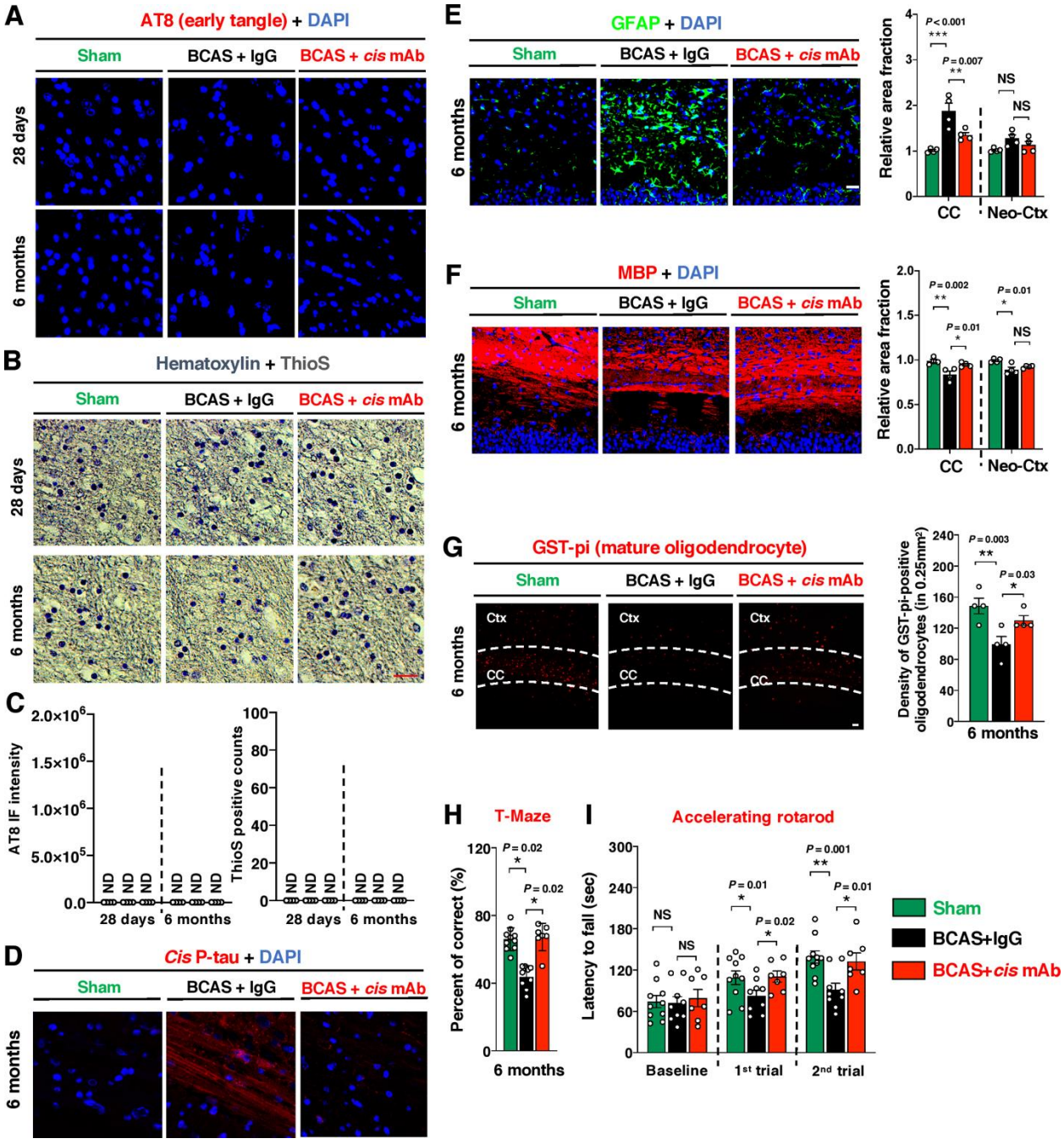

fig. S5. *Cis* mAb treatment of BCAS mice eliminates *cis* P-tau induction and inhibits neuroinflammation, demyelination, and oligodendrocyte loss 6 months after surgery. (**A-C**) Absence of AT8 and ThioS stained tangle-like structures in BCAS mouse brains at 28 days and 6

months. Representative images (**A** and **B**) and quantitation (**C**) are shown. (**D**) *Cis* P-tau IF staining in BCAS mice at 6 months after surgery. (**E-G**) *Cis* mAb treatment effect of BCAS mice 6 months after surgery, as examined by IF staining of GFAP (**E**), MBP (**F**), GST-pi-positive cells (**G**) with quantitation. (**H** and **I**) *Cis* mAb treatment effect of BCAS mice 6 months after surgery, as examined by percentage of correct choices in T maze (**H**) and latency to fall in accelerating rotatords (**I**). The data were presented as means ± SEM and the *p* values were calculated using one-way ANOVA with *post hoc* Dunnett's multiple comparison test. ND, Not detected; NS, Not significant; *, $p<0.05$; **, $p<0.001$; ***, $p<0.0001$.

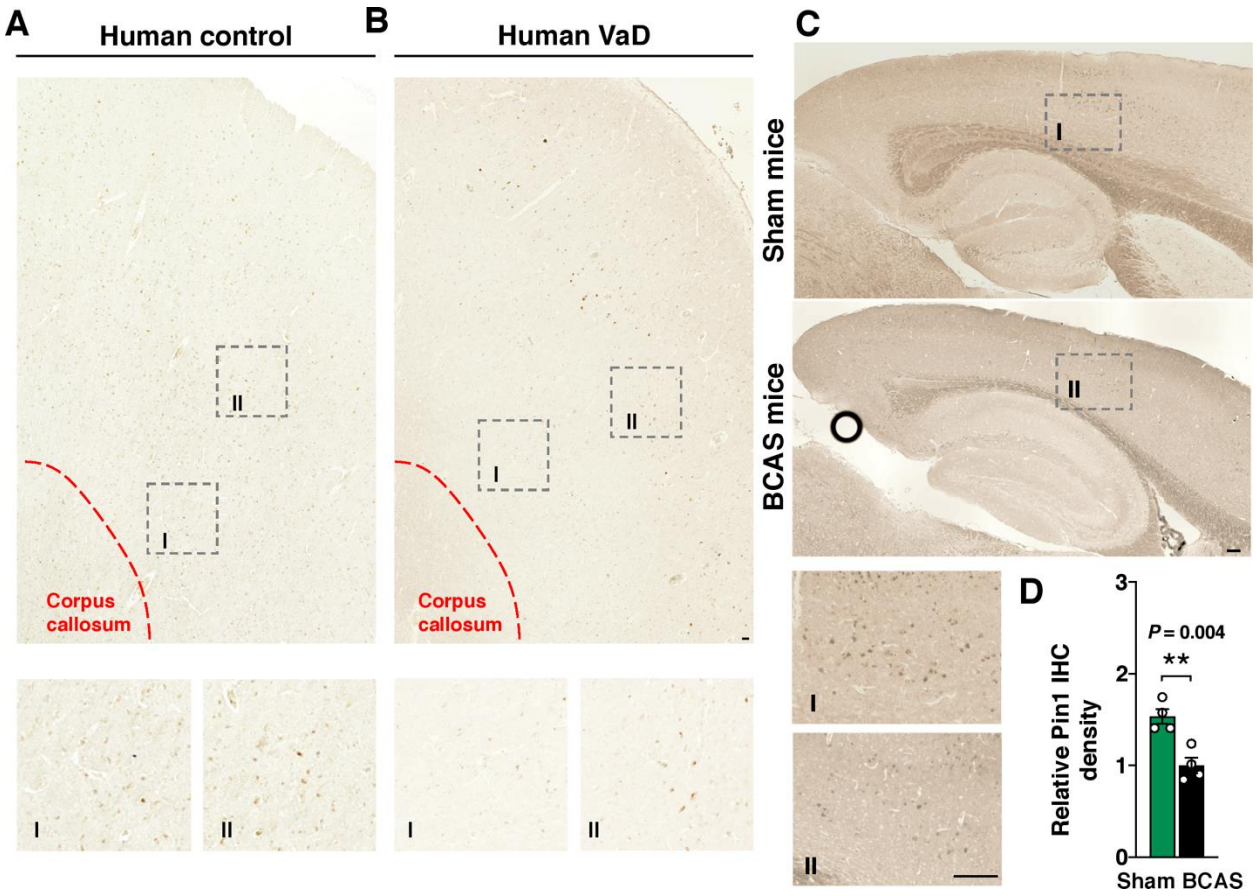

fig. S6. The sub-regions with low Pin1 expression in VaD human brains and in BCAS mouse brains. (**A** and **B**) Low power images of the sub-regions with low immunoreactivity of active Pin1 in VaD brain (**B**) as compared to an age-matched control (**A**). Lower panels are higher-magnification of the representative Pin1-labeled images comprised by the dashed rectangle with corresponding letters; Scale bar, 300 μm. (**C**) Brain sections of BCAS mice and sham controls were subjected with active Pin1 IF 28 days after surgery. Bottom left images are higher-magnification of the representative Pin1 labeled images comprised by the dashed rectangle with corresponding letters; Scale bar, 400 μm. (**D**) Quantitation of active Pin1 IF intensity in BCAS and sham mice 28 days after surgery. Data are presented as means ± S.E.M, and *p* values calculated using unpaired two-tailed Student's t-test. **, $p<0.01$.

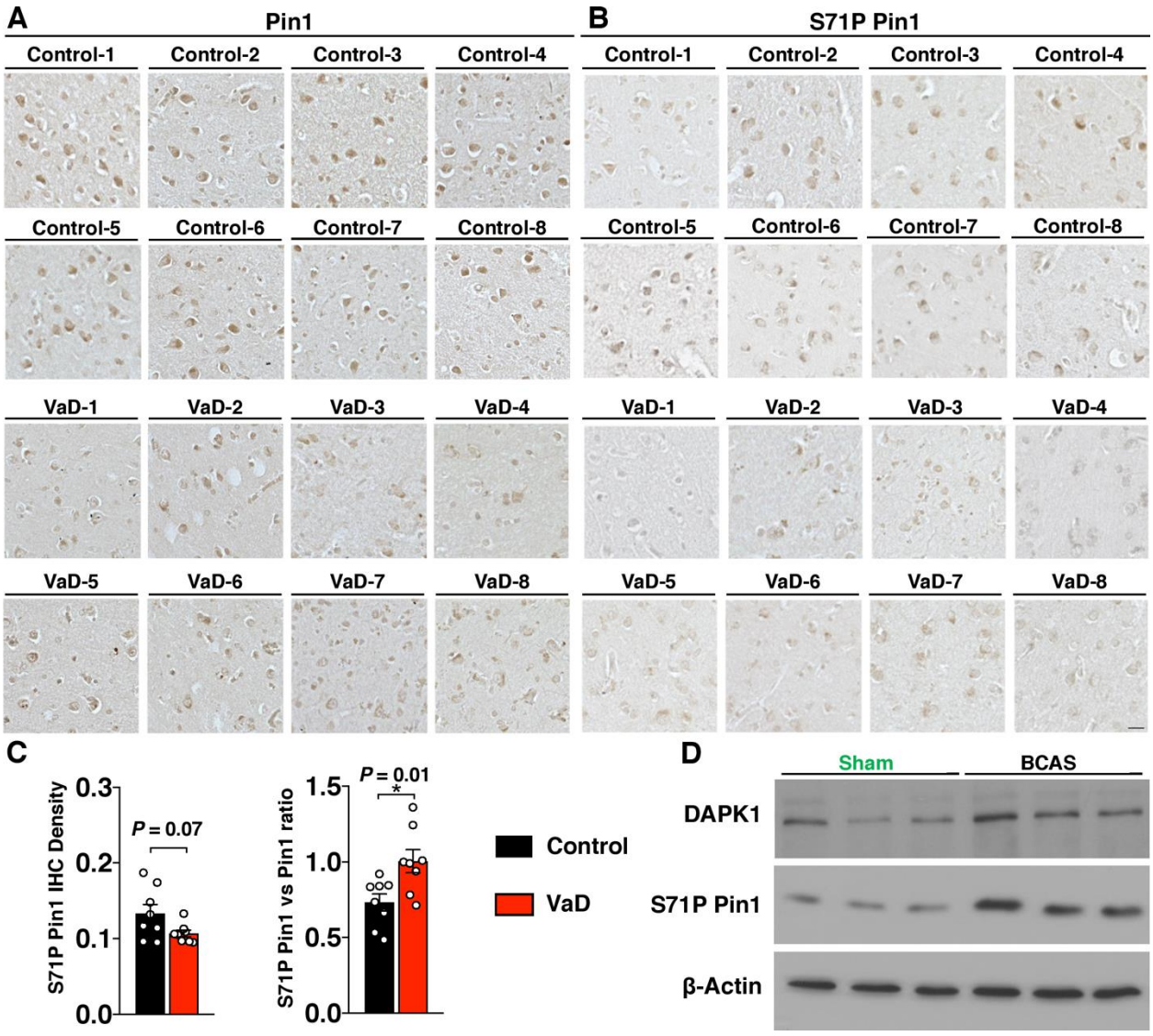

fig. S7. Reduced Pin1 expression, increased Pin1 S71 phosphorylation in VaD human brains and increased DAPK1 expression in BCAS mouse brains. (**A** and **B**) Immunohistochemistry of active Pin1 (**A**) and S71P Pin1 (**B**) levels in the cingulate cortex overlying the corpus callosum of human VaD brains compared with age-matched controls. Scale bar, 20 μm. (**C**) Quantitation of images from (**A** and **B**) and the ratio of S71P and active Pin1 are shown as means ± S.E.M. *p* values were calculated using unpaired two-tailed Student's t-test. (**D**) Immunoblotting of S71P Pin1 and DAPK1 in the cortex overlying the corpus callosum of mice 28 days after BCAS, as compared to sham littermate controls.

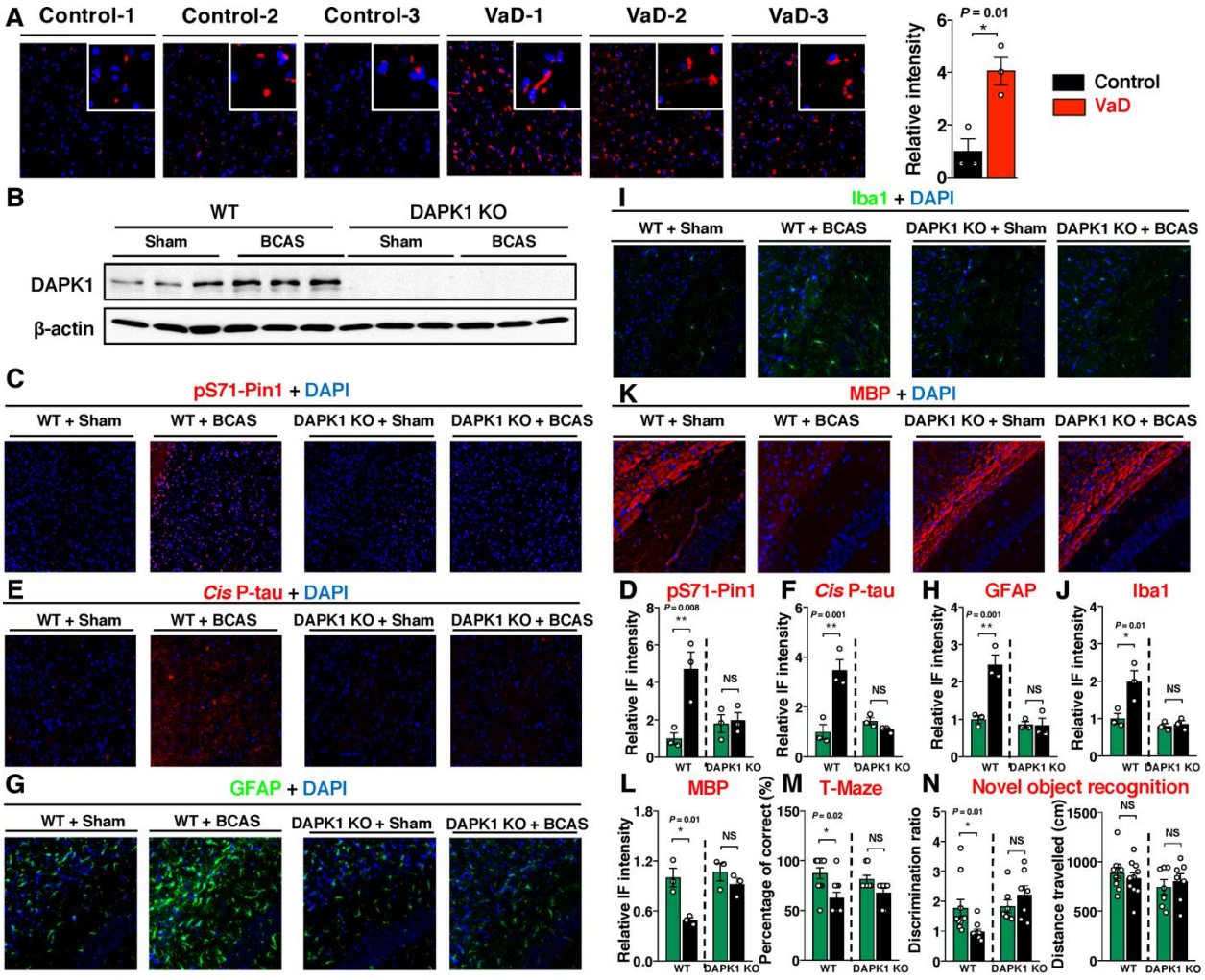

fig. S8. DAPK1 is activated in human VaD patients and BCAS mice, and DAPK1 KO blocks VCID-like pathology and brain dysfunction in BCAS mice. (**A**) Human (vascular dementia) VaD brain slices and aged-matched normal controls were immunostained with Pin1 P71 mAb and detected with bright-light microscopy. The relative intensity was quantified and shown as means ± S.E.M. (**B**) Immunoblotting of DAPK1 from the lysates of Ctx-CC of the WT and DAPK1 KO mice. (**C-L**) Effects of DAPK1 KO in the IF staining of Pin1 S71 phosphorylation (**C** and **D**), *cis* P-tau (**E** and **F**), GFAP **(G** and **H)**, Iba1 **(I** and **J)** and MBP **(K** and **L)** in the Ctx-CC subregions at 28 days after BCAS surgery, as compared to sham controls. (**M** and **N**) Effects of DAPK1 KO in the working memory deficits in BCAS mice, as analyzed by percentage of correct choices in

the T-maze **(M)** and discrimination ratio in the novel object recognition **(N)** tests at 28 days after BCAS. NS: not significant. The *p* values were calculated using one-way ANOVA with *post hoc* Dunnett's multiple comparison test. NS, not significant, *$p<0.05$, **$p<0.01$.

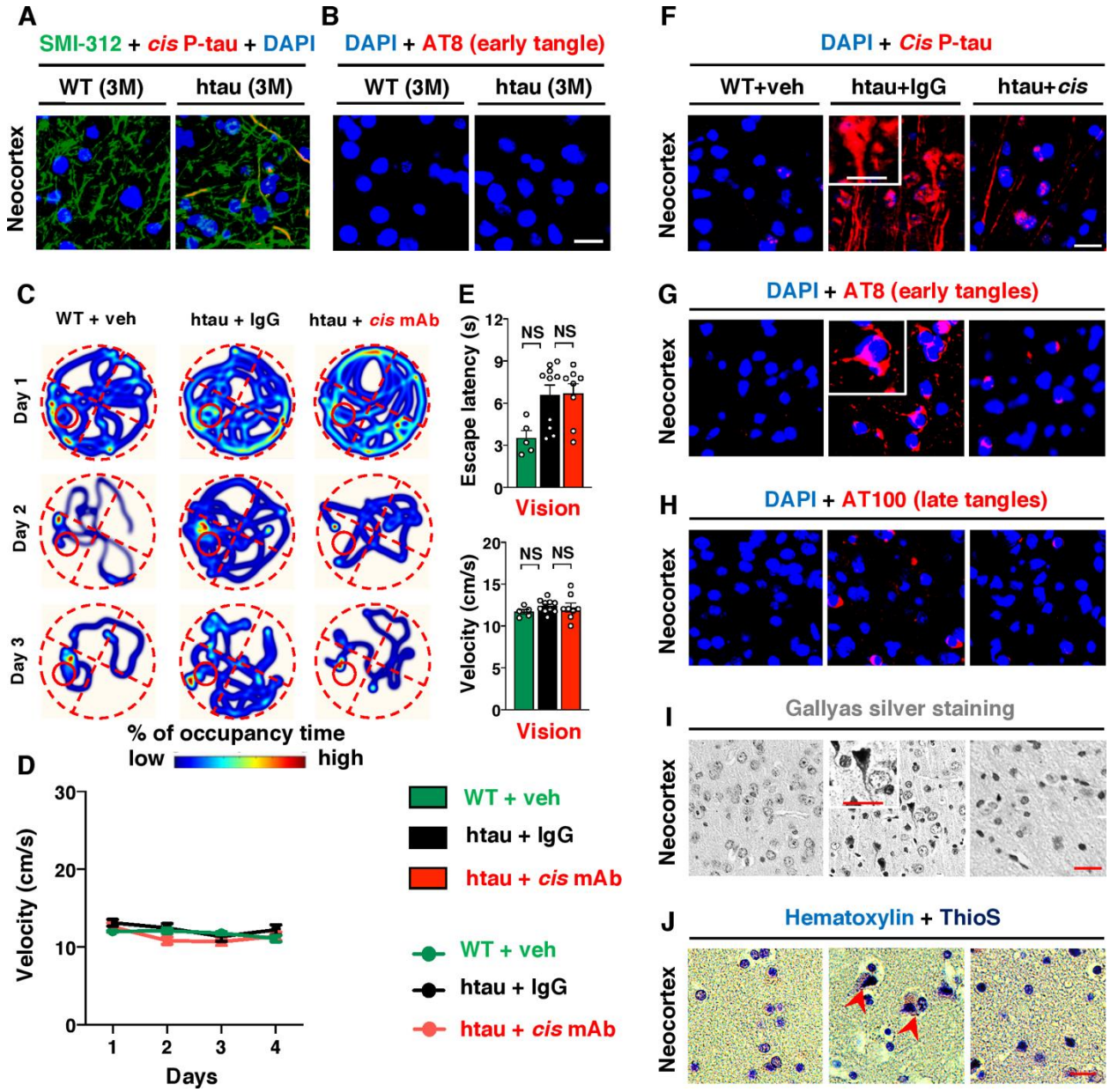

fig. S9. *cis* P-tau elimination in young htau mice prevents the development of NFT-like pathology and functional impairments. (**A** and **B**) Three-month-old (3M) htau mouse brain sections were subjected to double IF staining with axon marker SMI-312 and *cis* P-tau (**A**); or single IF with early tangle marker AT8 (**B**) along with DAPI. (**C-E**) Results of the Morris water maze after 8 months of *cis* mAb treatment in htau mice showing trajectories (**C**) and velocity (**D**)

in the acquisition trial, as well as the motivation of finding the platform in vision trial between the groups (**E**). NS: not significant. The data were presented as means ± SEM. The *p* values were calculated using one-way ANOVA with *post hoc* Dunnett's multiple comparison test. (**F-J**) *Cis* mAb treatment effect of *cis* P-tau (**F**), the development of tangle-like pathologies detected by AT8 antibody (**G**), AT100 antibody (**H**), Gallyas silver staining (**I**)**,** and ThioS staining (**J**) in neocortex of htau mice compared with IgG controls. Higher magnification images of representative structures are provided in the insets. Neurofibrillary tangles are indicated with red arrows in thioflavin S staining.

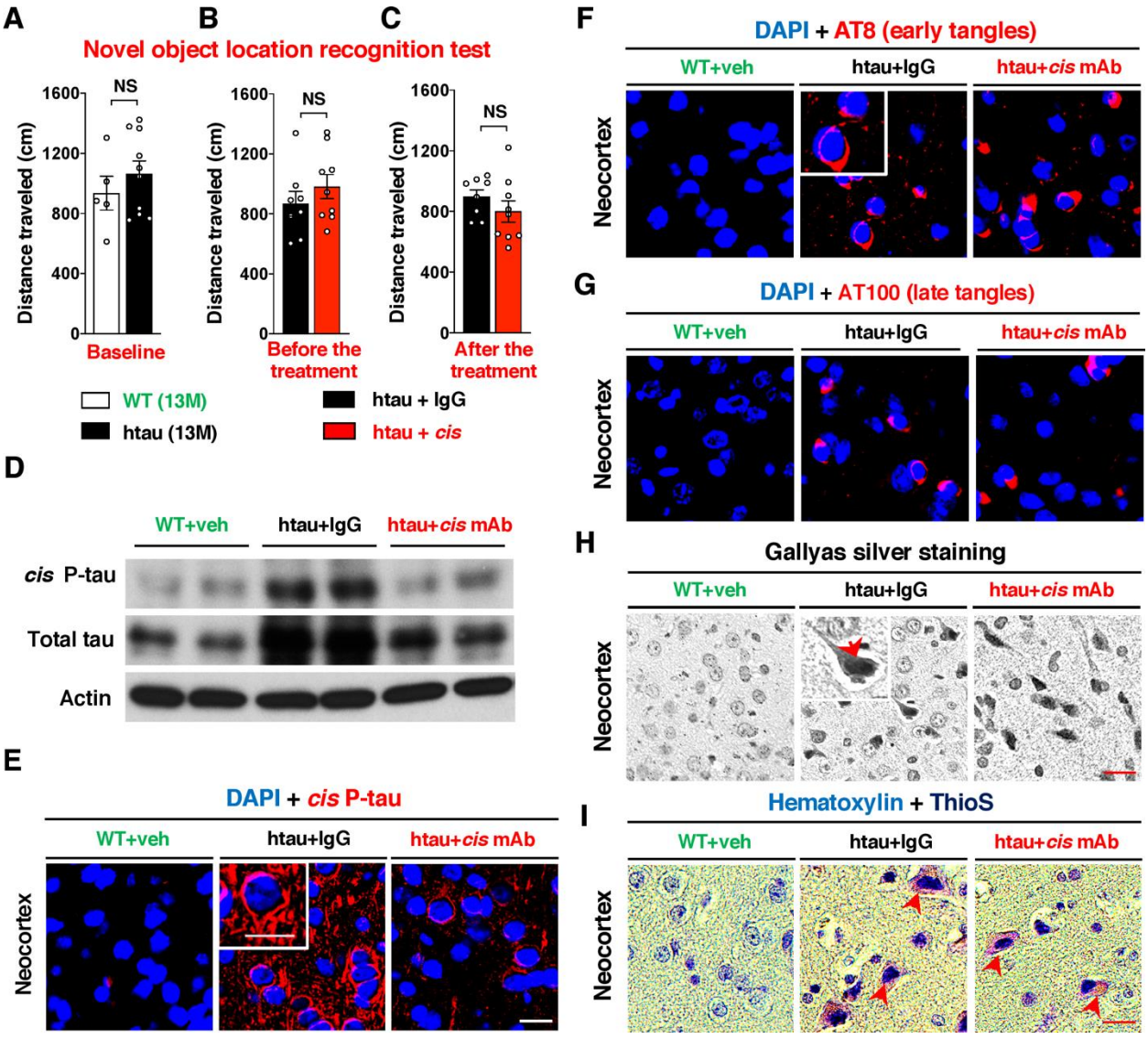

fig. S10. *cis* mAb treatment of symptomatic, aged htau mice attenuates neurodegeneration and improves cognitive impairment without clearance of NFT-like pathology. (**A-C**) Distance traveled in the novel object recognition tests between the 13-month-old htau mice and WT controls (**A**), as well as htau mice before (**B**) and after treatment (**C**). NS: not significant. The data were presented as means ± SEM. The *p* values were calculated using unpaired two-tailed Student's t-test. (**D**) *cis* mAb treatment effect of *cis* P-tau and total tau in the hippocampus of htau mice, with

WT vehicle controls. (**E**) *Cis* mAb treatment effect of *cis* P-tau in the neocortex, as assessed by IF staining of *cis* P-tau. (**F-I**) *Cis* mAb treatment effect of tangle-like pathologies detected by IF staining with AT8 antibody (**F**), AT100 antibody (**G**), Gallyas silver staining (**H**)**,** and ThioS staining (**I**) in the neocortex of the mice, as visualized by confocal microscopy. Higher magnification images of representative structures are provided in the insets. Neurofibrillary tangles are indicated with red arrows in the gallyas silver and thioflavin S staining. Scale bar, 20 μm.

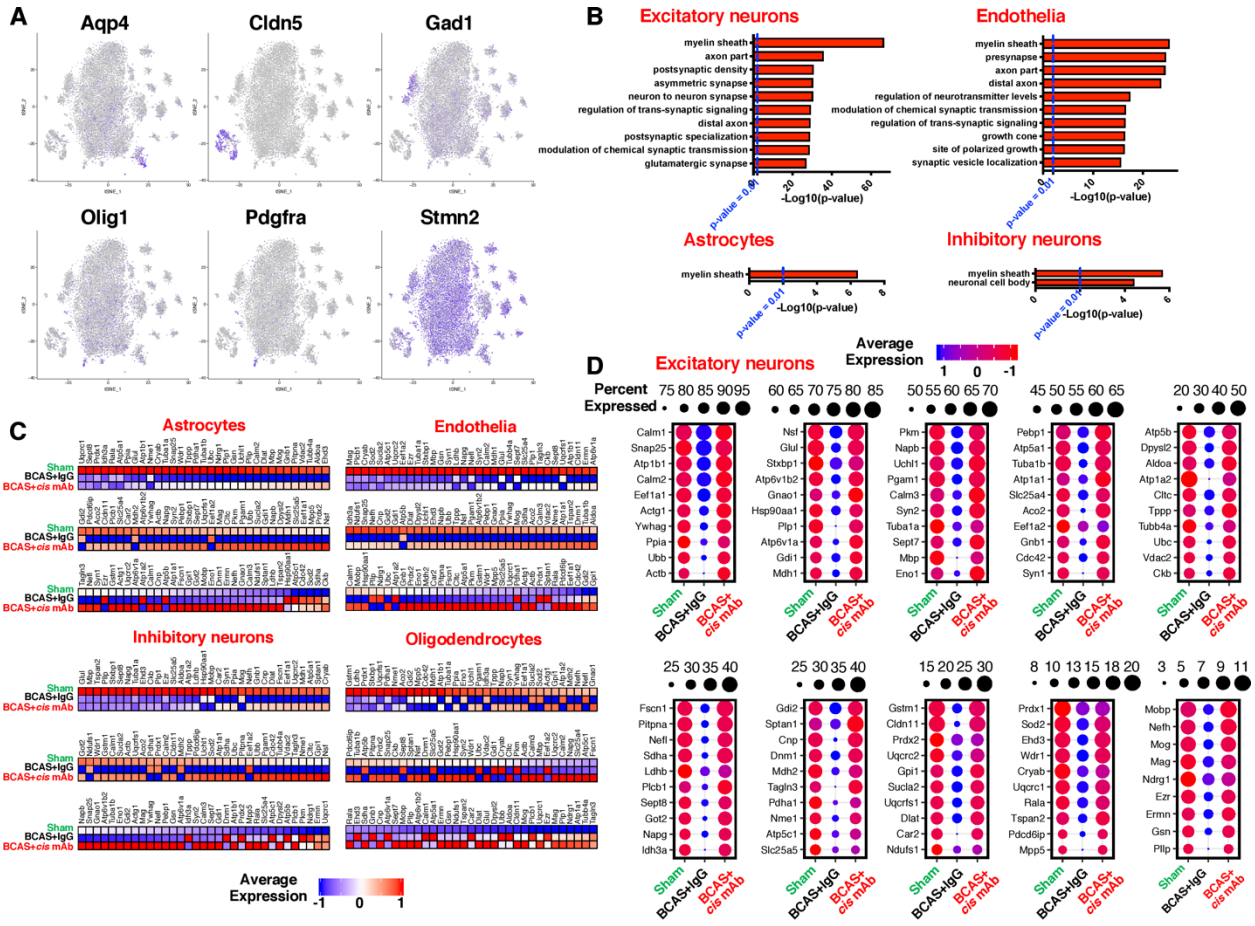

fig. S11. BCAS induced transcriptomic changes widely associated with demyelination in diverse cell types, the vast of majority of which are recovered by *cis* mAb. (**A**) Expression patterns of cell-type specific marker genes across cell clusters in BCAS scRNA-seq experiments (Sham, BCAS+IgG, BCAS+*cis* mAb). Expression patterns for astrocyte marker Aqp4, endothelia marker Cldn5, inhibitory neuron marker Gad1, oligodendrocyte markers Olig1 and Pdgfra and neuronal marker Stmn2 are shown in heatmaps. Each cell is color coded by the relative expression of the indicated gene from minimal (grey) to maximal (blue). (**B**) Enriched gene-ontology terms in the most down-regulated DEGs in diverse cortical cell types in BCAS mice. (**C**) Heatmaps for average expression of individual genes associated with myelin sheath gene ontology term in BCAS

mice treated with *cis* mAb or IgG control, referencing to sham littermates. (**D**) Dotplots color coded with average expression and sized with the percentage of cells that express genes associated with myelin sheath gene ontology term in BCAS mice treated with *cis* mAb or IgG control, referencing to sham littermates. The 99 myelin sheath genes were ranked from the most highly expressed (top left) to the least expressed (bottom right) in dot plots using Seurat 3. The color scales from low relative expression (blue) to high relative expression (red). The dot size represents the percentage of cells that express the gene.

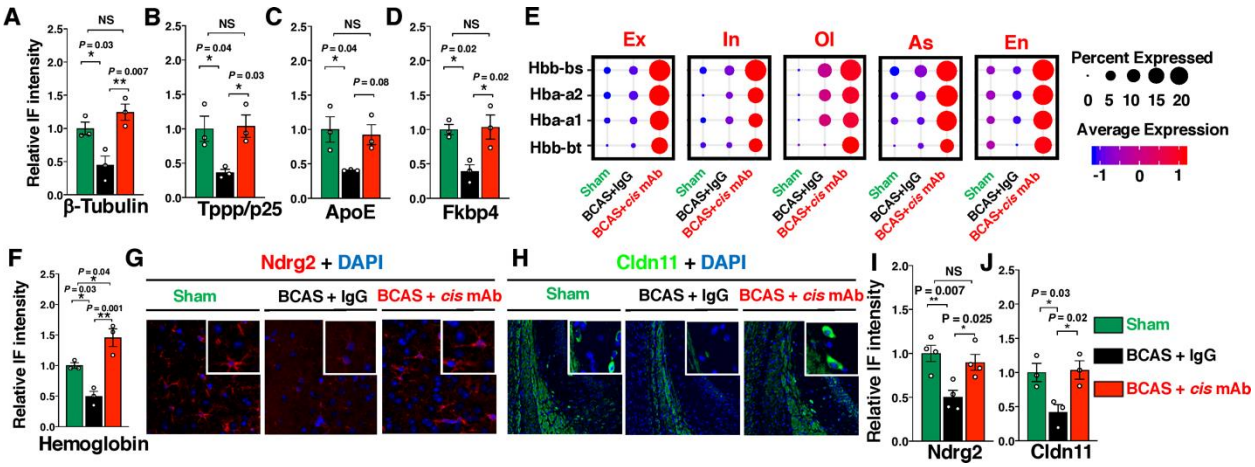

fig. S12. BCAS induced transcriptomic changes and *cis* mAb induced hemoglobin expression are validated by immunofluorescence staining. (**A-D**) Relative IF intensity quantitation of ß-Tubulin **(A)**, Tppp/p25 **(B)**, ApoE **(C)** and Fkbp4 **(D)**. (**E**) Dotplots showing average expression of hemoglobin genes and percentage of cells that express the genes in different cell types. (**F**) Relative IF intensity quantitation of hemoglobin. (**G-J**) Validation of DEGs by immunofluorescence staining of Ndrg2 **(G)** and Cldn11 **(H),** and quantitation of the relative immunofluorescence intensity **(I** and **J)**. The bargraphs in this figure were presented as means ± SEM, and the *p* values were calculated using one-way ANOVA with *post hoc* Dunnett's multiple comparison test. *p<0.05; **p<0.01.

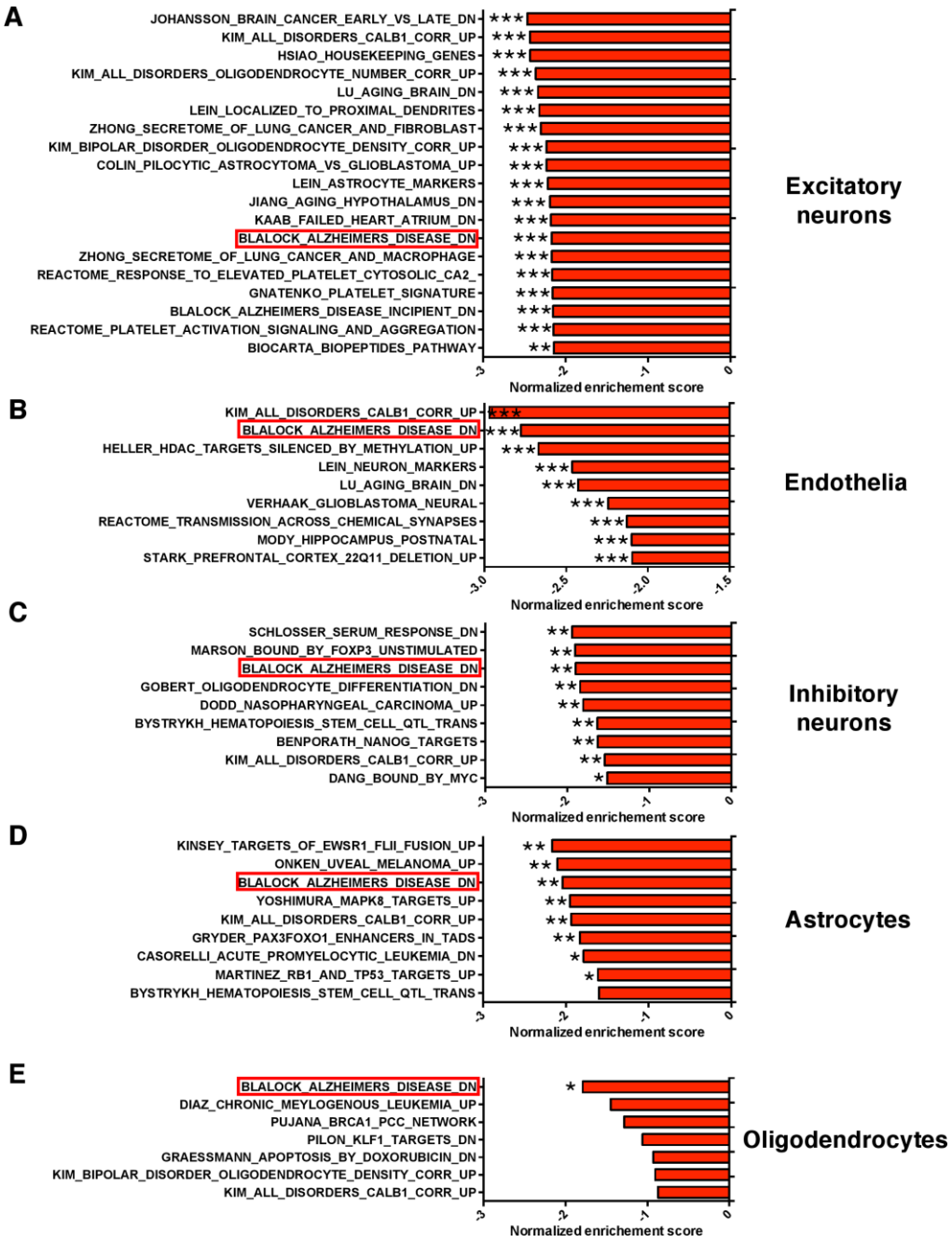

fig. S13. Gene-set enrichment analyses of cell-type specific differentially expressed genes for the curated gene sets (MSigDB C2). Normalized enrichment scores for top 10 enriched gene sets are plotted as bargraphs, with *p* values indicated as *, $p < 0.05$, **, $p < 0.01$, ***, $p < 0.001$.

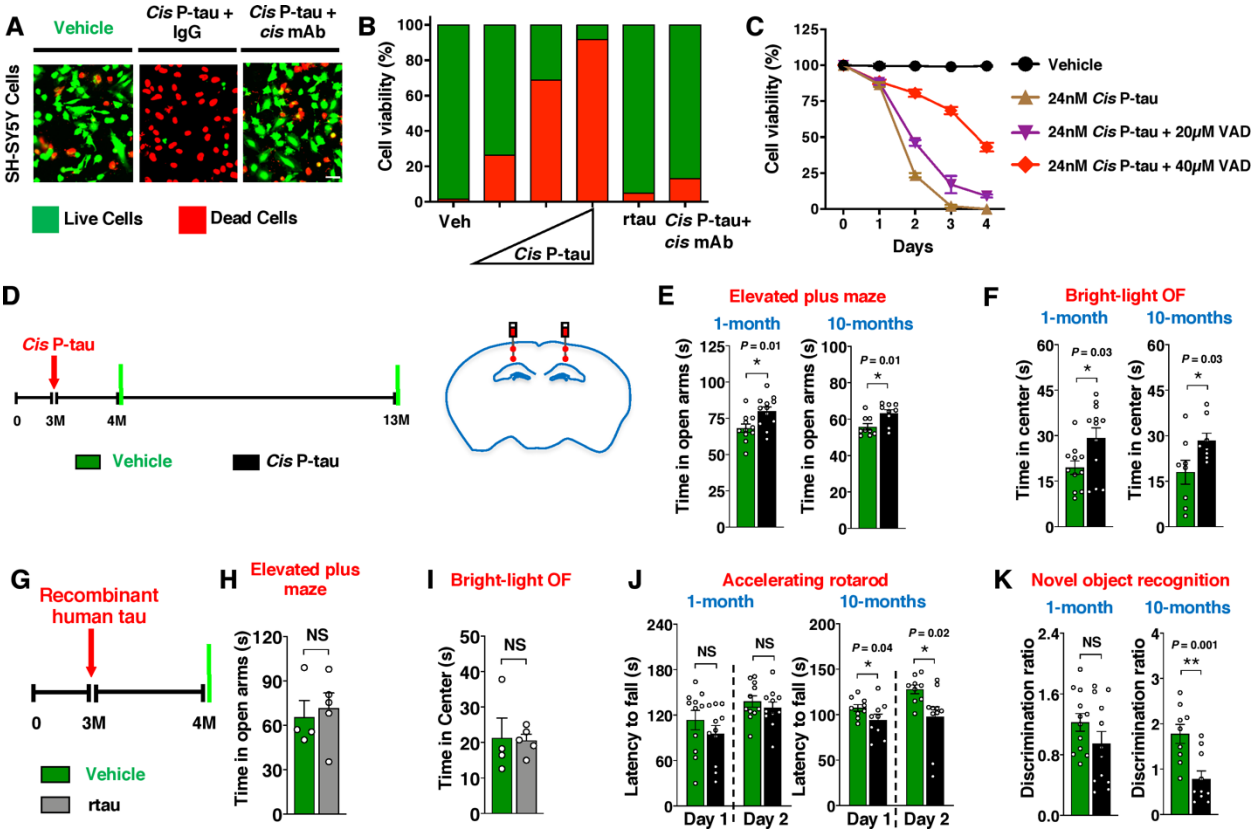

fig. S14. Intra-cortical injection of purified *cis* P-tau causes neuronal death in vitro and behavioral changes in mice. (**A-C**) Dose-dependent neurotoxicity of purified *cis* P-tau to growing SH-SY5Y cells (10ng, 20ng, 40ng) in the presence or absence of Z-VAD-FMK Inhibitor for 48 hours, followed by live and dead cell assay. (**D**) Three-month-old (3M) WT mice were stereotaxically microinjected with purified *cis* P-tau or control vehicle bilaterally into the upper & lower layer of the neocortex according to the experimental setup (Red arrow, stereotaxic injection; green lines, functional assays). (**E** and **F**) Risk-taking behavior of mice at 1 or 10 months after *cis* P-tau injection, assessed by time in open arms in elevated plus maze (**E**) and time in center in the bright light open field assays (**F**). (**G-I**) Three-month-old (3M) WT mice were stereotaxically infused with rtau (0.4 μg/μl) or vehicle bilaterally into the upper & lower layer of the neocortex. Red arrow, stereotaxic injection; green lines, functional assays. We analyzed the risk-taking behavior at 1-month after the injection by elevated plus maze **(H)** and bright-light open field **(I)**.

(**J** and **K**) Progressive effect of *cis* P-tau injection on the accelerating rotarod (**J**) and novel object location recognition (**K**). The data were presented as means ± SEM. The *p* values were calculated using unpaired two-tailed Student's t-test. NS: not significant.

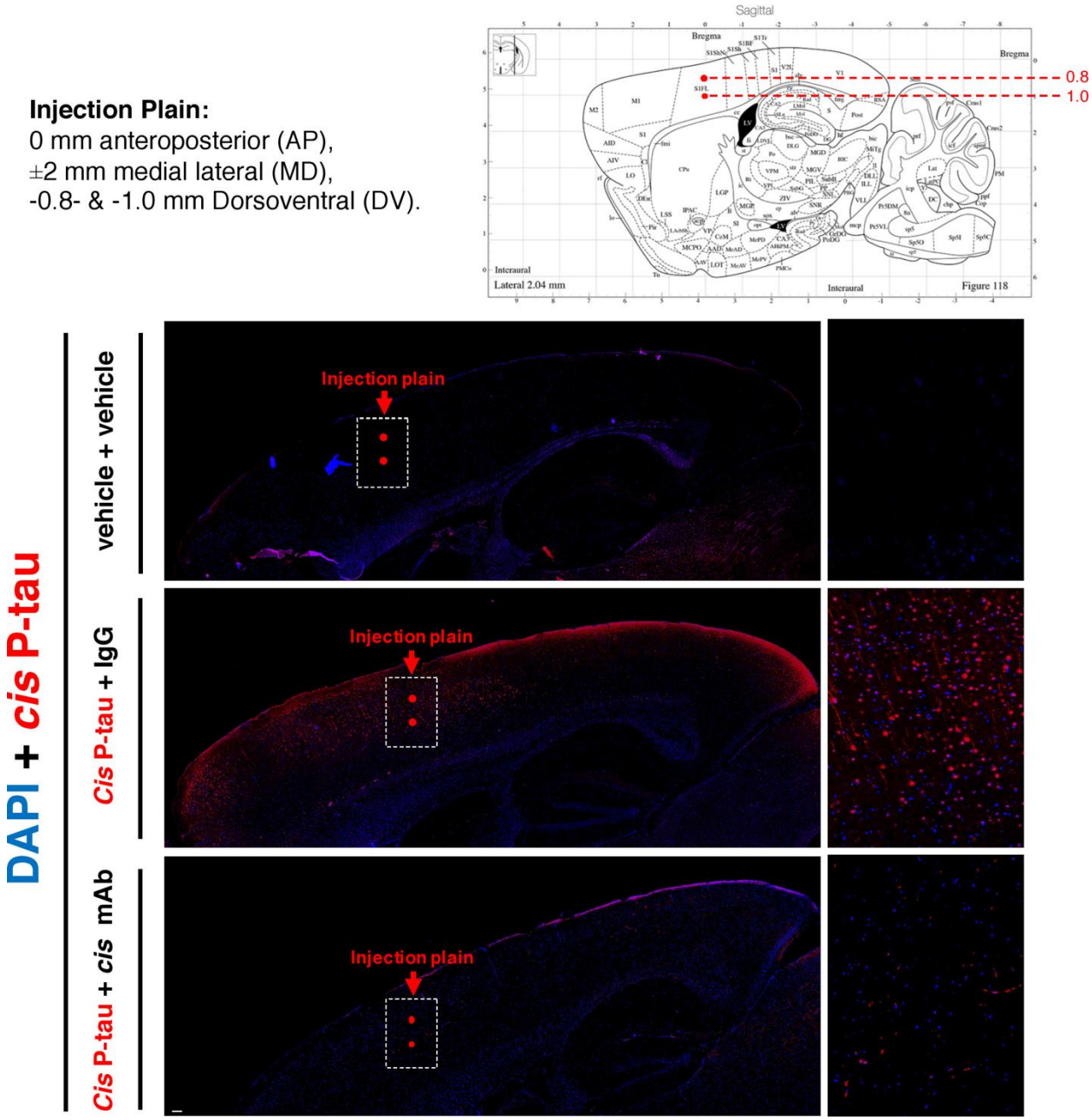

fig. S15. Progressive accumulation of *cis* P-tau in WT mice injected with purified *cis* P-tau. Stereotaxic coordinates were determined from "The Mouse Brain in Stereotaxic Coordinates (Paxinos and Franklin)". Three-month-old (3M) WT mice underwent stereotaxic intra-cortical injection of 2µL purified soluble *cis* P-tau or vehicle (0.1 µg/µl), and were continuously subjected

to treatment regimens of *cis* mAb, IgG isotype or vehicle controls over 5-months, followed by immunofluorescence staining of *cis* P-tau immunoreactivity in whole brain sections to detect *cis* P-tau accumulation over the cortex at 10-months after injection. Inset images (right) are high magnifications of representative areas. Scale bar, 400 μm.

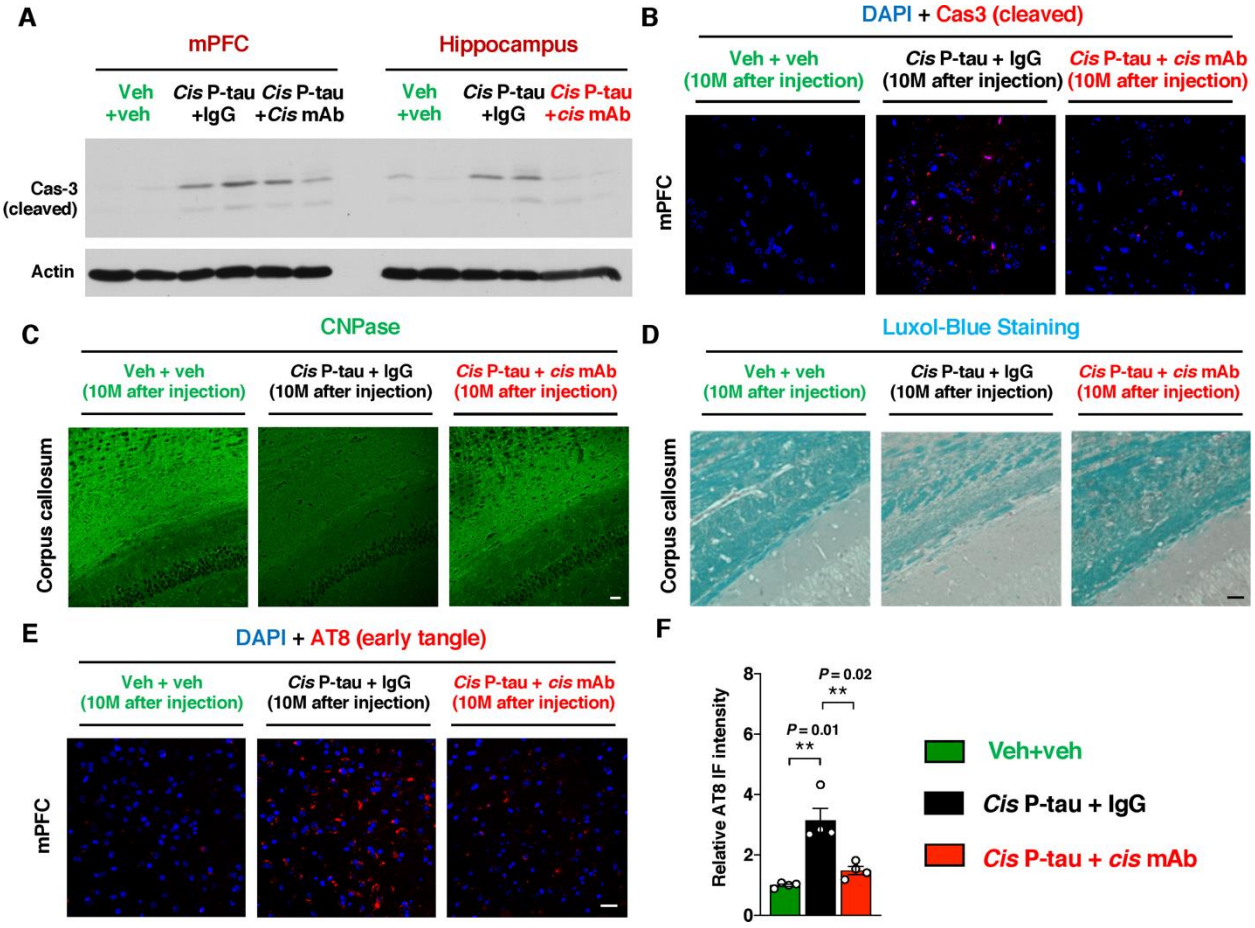

fig. S16. Intra-cortical injection of purified *cis* P-tau induces neuronal death, demyelination and tau-related pathology in vivo. Three-month-old (3M) WT mice underwent stereotaxic intra-cortical injection of 2μL purified *cis* P-tau or vehicle (0.1 μg/μl), and were continuously subjected to treatment regimens of *cis* mAb, IgG isotype or vehicle controls over 5-months, followed by immunoblotting **(A)** and immunofluorescence **(B)** staining of cleaved caspase-3 immunoreactivity in neocortex and hippocampus to detect relative apoptotic activity; CNPase antibody immunostaining **(C)** and Luxol-Blue staining **(D)** to detect demyelination; and AT8 antibody immunostaining to detect early-tangle like epitopes **(E)** and its statistical data for IF signal of medial prefrontal cortex **(F)** at 10-months after injection. Scale bar, 20 μm. mPFC: Medial

prefrontal cortex. The data were presented as means ± SEM. The p values were calculated using one-way ANOVA with *post hoc* Dunnett‘s multiple comparison test. *, $p<0.05$; **, $p<0.01$.

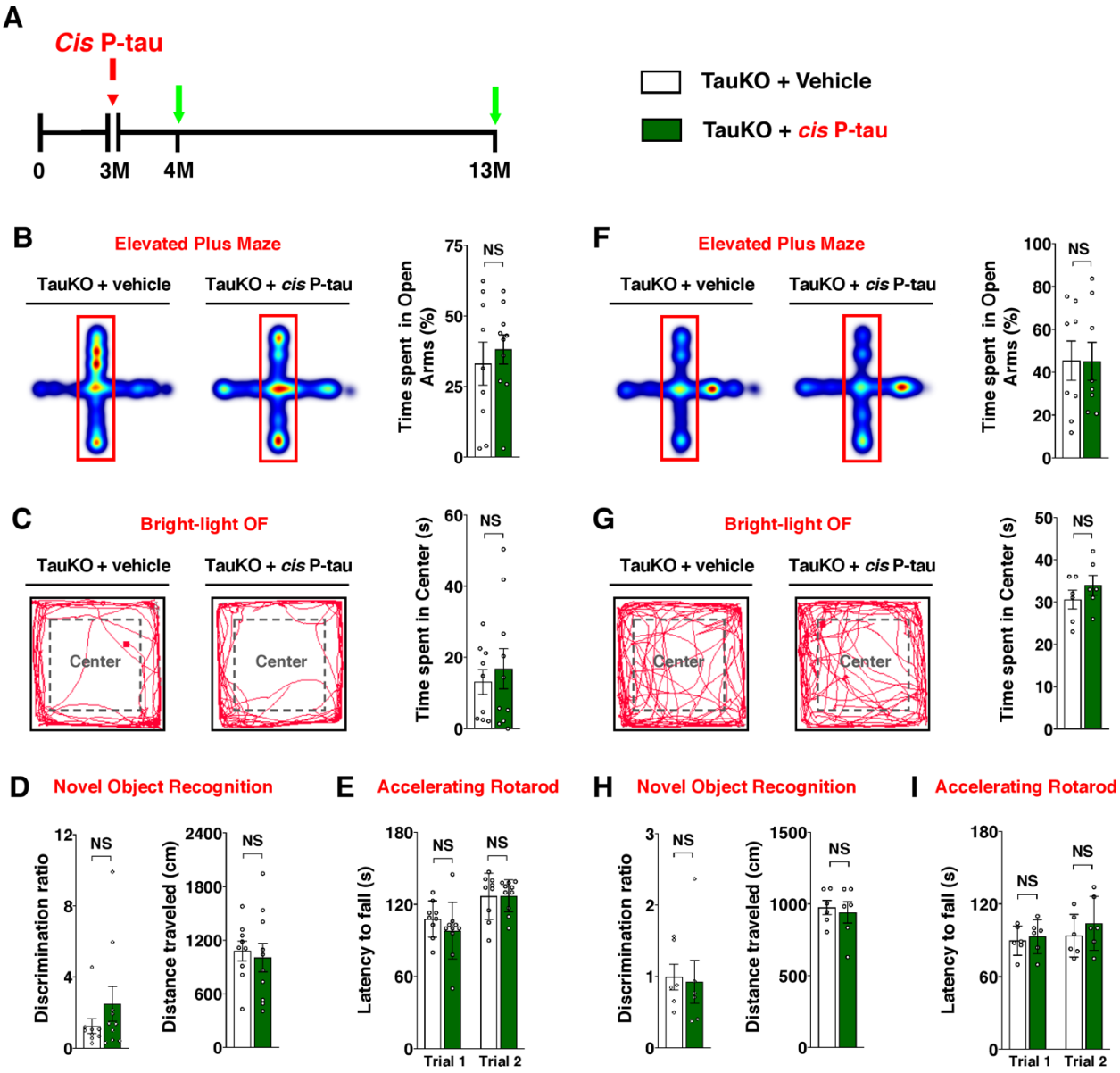

fig. S17. Cortical injection of purified *cis* P-tau has no significant behavioral effect in TauKO mice. (**A**) Experimental setup. 2µL of purified *cis* P-tau (0.1 µg/µl) or vehicle control were injected bilaterally into the upper (DV, -0.8mm) & lower (DV, -1.0mm) layer of the neocortex of three-month-old TauKO mice (red arrows). Functional assays are indicated by green arrows. (**B-I**) Assessment of behavioral changes of *cis* P-tau or vehicle injected Tau KO mice using the Elevated

plus maze **(B, F)** , bright-light open field **(C, G)**, novel object recognition **(D, H)** and Accelerating rotarod **(E, I)** tests at 1 month **(B-E)** and 10 months **(F-I)** after the injection. NS: not significant. 6-10 mice per group were included in each of the behavioral tests. The data were presented as means ± SEM. The *p* values were calculated using unpaired two-tailed Student's t-test.

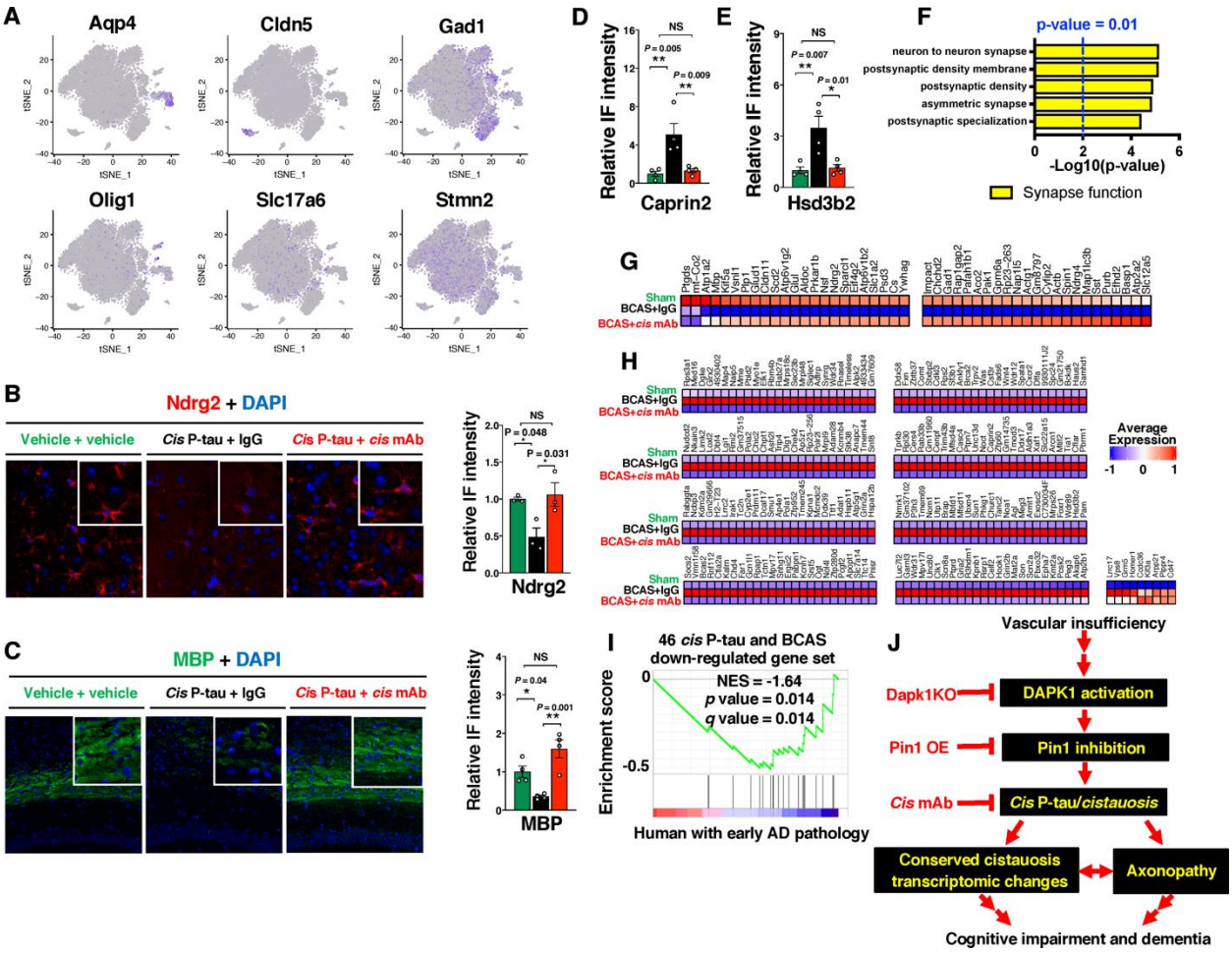

fig. S18. Injected *cis* P-tau induces the conserved transcriptomic changes found in mouse VCID and human AD with early pathologies. (**A**) Expression pattern of cell-type specific marker genes across cell clusters in mice stereotaxically injected with cis P-tau or vehicle control. Expression patterns for astrocyte marker Aqp4, endothelia marker Cldn5, inhibitory neuron marker Gad1, oligodendrocyte markers Olig1, excitatory neuronal markers Slc17a6 and Stmn2 are shown in heatmaps. Each cell is color coded by the relative expression of the indicated gene from minimal (grey) to maximal (blue). (**B-E**) Validation of some scRNA-seq predicted DEGs in *cis* P-tau injected mice by immunofluorescence staining of Ndrg2 **(B)** and Mbp (**C**) and quantitation of the relative fluorescence intensity. Relative fluorescence intensity for Caprin2 and Hsd3b2 are also

quantified and shown in **(D, E)**, respectively. The data were presented as means ± SEM. The p values were calculated using one-way ANOVA with *post hoc* Dunnett's multiple comparison test. *p<0.05, **p<0.01. (**F**) The 209 commonly up-regulated genes between *cis* P-tau injection and BCAS are enriched in genes related to Synapse function. The *p*-values for the enriched gene-ontology terms are showed in bar graphs. (**G** and **H**) *Cis* mAb treatment effect of the 46 genes that are commonly down-regulated by BCAS and *cis* P-tau injection **(G)** and 209 genes that are commonly up-regulated by BCAS and *cis* P-tau injection **(H)** in BCAS mice cortex are shown in heatmap. (**I**) Negative enrichment of the 46 commonly down-regulated genes by BCAS and *cis* P-tau injection in genes down-regulated in patients with early AD pathology. (**J**) A schematic model for Pin1 and *cis* P-tau in VCID. Neurovascular insufficiency activates DAPK to inhibit Pin1, which fails to repress the induction of *cis* P-tau. *Cis* P-tau induction can be attenuated by *cis* mAb treatment, Pin1 overexpression (OE) or DAPK knockout (KO). If not attenuated, *cis* P-tau induces the conserved transcriptomic changes, cistauosis and axonopathy, which may lead to cognitive impairment and dementia. Double arrow indicate possible involvement of multiple molecular events in between.

Table S1. The clinical information of patients with VaD and healthy controls.

Table S2. Differentially expressed genes in five major cortical cell types from BCAS mice.

Table S3. Gene-ontology terms enrichment in the down-regulated genes in the BCAS cortical excitatory neurons.

Table S4. Differentially expressed genes in five cortical cell types from *cis* P-tau injected mice.

Table S5. Gene-ontology terms enrichment in the down-regulated genes in the BCAS cortical excitatory neurons.

Movie S1. MWM probe trial (WT+vehicle)

Movie S2. MWM probe trial (htau+IgG)

Movie S3. MWM probe trial (htau+cis mAb)

Data file S1: Raw data

Data file S2: Uncropped Western blot films